

Proceedings

1 Reclaiming of ground tire rubber by primary and secondary amines as the 2 devulcanizing agents †

3 Selly Mitra Mailanda¹, and Rathanawan Magaraphan^{1,2}

4 ¹The Petroleum and Petrochemical College, Chulalongkorn University, Bangkok, Thailand.

5 ²Center of Excellence in Green Materials for Industrial Application, Faculty of Science,
6 Chulalongkorn University, Bangkok, Thailand.

7 *rathanawan.k@chula.ac.th

8 †Presented at Asia Rubber and Elastomer Federation International Conference AREF-IC 2024,
9 AVANI+ Khao Lak, Phang-Nga, Thailand on Feb. 27-Mar.1, 2024.

10 **Abstract:**

11 Recycling end-of-life tires is an environmental challenge due to their high-performance
12 characteristics. In this study, varying amounts of caprolactam and hexamethylenediamine are utilized
13 for the first time to facilitate the devulcanization of rubbers. The primary or secondary amine groups
14 present in caprolactam and hexamethylenediamine can cleavage crosslink bonds, thereby increasing
15 the degree of devulcanization, and sol fraction and decreasing the crosslink density of reclaimed
16 rubbers (RRs). Using 100 phr ground tire rubber (GTR) prepared at 180°C in 75 minutes with
17 processing oil and adding caprolactam and hexamethylenediamine prove that amine groups impacted
18 RRs with different devulcanization degrees. Increasing the amounts of caprolactam exhibits the
19 highest devulcanization degree of 77.7%, surpassing commercial TEPA (70.8%) and exceeding that
20 of thermally devulcanized GTR. However, with hexamethylenediamine, the degree of devulcanization
21 is lower at 58.0%. Torque measurements from MDR show that increasing the amounts of caprolactam
22 and hexamethylenediamine results in lower torque (0.95 and 0.90 dN.m) compared to TEPA (1.19
23 dN.m). In conclusion, caprolactam, containing the amine with an α -H atom, proves its effectiveness as
24 a devulcanizing agent. However, both caprolactam and hexamethylenediamine have the potential to
25 be devulcanizing agents.

26
27 **Keywords:** caprolactam; devulcanizing agent; hexamethylenediamine; reclaimed rubber;
28 rubber recycling.
29

30 **1. Introduction**

31 Tires contribute to about 70% of global rubber production and every year, roughly
32 800 million (~10 million tons) of trash tires are wasted globally (Asaro et al., 2018).
33 Devulcanization of rubber waste is a proposed method of recycling waste tire rubber that
34 involves the cleavage of intermolecular carbon-sulfur and sulfur-sulfur bonds, resulting in

35 shorter polymer chain lengths than the original, and thus worse rubber characteristics
36 (Thaicharoen et al., 2010). To effectively devulcanize, sulfide compounds, such as diphenyl
37 disulfide, are usually utilized at temperatures of 200°C or higher. This may result in higher
38 energy usage and possible rubber thermal degradation (Guo et al., 2024). Based on the initial
39 patent in 2003 by (van et al., 2003) amines may assist in radical-dominated high-temperature
40 devulcanization.

41 Hexadecylamine was used by Dijkhuis et al. (Dijkhuis et al., 2008) To devulcanize
42 EPDM during thermal devulcanization, they found a 50% reduction in crosslink density.
43 Tetraethylenepentamine (TEPA), and other amine substances have also been used in
44 conjunction with mechanical or ultrasonic devulcanization, enabling the treatment to be
45 carried out at lower temperatures (Sutanto et al., 2006). Based on this consideration,
46 exploring amine compounds as a devulcanizing agent for rubber reclamation, gave rise to this
47 research idea, caprolactam, and hexamethylenediamine. They are promoted as an innovative
48 devulcanizing agent with the potential to devulcanize waste tire rubber.

49 The purpose of this study is to investigate the devulcanization mechanism of amine
50 groups of caprolactam and hexamethylenediamine (HMDA) on ground tire rubbers, as well
51 as to optimize the process reattachment after the positively charged sulfur produced by sulfur-
52 breaking is linked with the amine from the devulcanizing agent. This study addresses an
53 effort on a devulcanization process employing amine compounds, focusing on sol fraction
54 and crosslink density, which can directly indicate the degree of devulcanization. This research
55 prioritizes simplicity, employing environmentally friendly sources and chemicals, and
56 minimizing energy consumption.

57 **2. Experimental**

58 *2.1 Materials*

59 The materials used in the devulcanization process include tread rubber powders from
60 waste tires (obtained from Union Commercial Development Co., Ltd), the particle size of the
61 rubber powders is mainly distributed 20 mesh. Caprolactam, hexamethylenediamine, and
62 tetraethylenepentamine (TEPA) were purchased from Sigma Aldrich. Alpha-terpineol is a
63 processing oil purchased from beScents.

64 2.2. Experimental procedure

65 2.2.1. Devulcanization process

66 Ground tire rubber (GTR) (100 phr) was combined with 10 phr of processing oil and
67 various concentrations of caprolactam and hexamethylenediamine (5; 10; 15 phr) at room
68 temperature (D-CaproGTRs and D-HMDAGTRs), and for controlling 10 phr of only TEPA
69 was added to GTR (D-TEPAGTR). The devulcanization procedure was then performed for 75
70 minutes using an internal mixer set to 70 rpm and 180°C. Following devulcanization, the
71 sample was removed from the internal mixer and chilled immediately in a water bath. The
72 sample would next be rolled through the two-roll mill before being compressed (Wang et al.,
73 2023).

74 2.3 Measurements and Characterizations

75 The sol fraction was evaluated by Soxhlet extraction (Alonso Pastor et al., 2021). A
76 rubber sample with a certain mass was extracted in acetone for 12 hours, dried at 80°C to a
77 constant weight (m_1), and further extracted in toluene for 16 hours before being vacuum-dried
78 at 80°C to a consistent weight (m_2). The sol fraction is calculated by:

$$79 \quad S_f = (m_1 - m_2)/m_1 \quad (1)$$

80 The devulcanizing ratio, which represents the degree of devulcanization, is computed
81 by:

$$82 \quad Rd = (v_{e1} - v_{e2})/v_{e1} \quad (2)$$

83 The crosslink density of a rubber sample was determined using the equilibrium
84 swelling method and the Flory-Rehner equation (Shi et al., 2012). The sample was Soxhlet-

85 extracted in acetone for 12 hours, dried at 80°C to a constant weight (m_i), and then swelled in
86 toluene for 72 hours at room temperature. After removal from toluene, it was weighed (m_t)
87 and dried to a constant weight (m_d) at 80°C. Then, the crosslink density of the rubber sample
88 is calculated by:

$$89 \quad v_e = \frac{-[\ln(1-V_r) + V_r + \chi V_r^2]}{V_l (V_r^{1/3} - V_r/2)} \quad (3)$$

$$90 \quad V_r = \frac{m_d/\rho_d}{m_d/\rho_d + m_s/\rho_s} \quad (4)$$

$$91 \quad m_s = m_t - m_d \quad (5)$$

92 The torque profile was evaluated by Moving Die Rheometer (CEAST 5000) at 100°C,
93 the sample was prepared at approximately 4.5 cm³ or at least the minimum size of the cone to
94 cover all the cone and plate surface.

95 SEM observation with a scanning electron microscope Hitachi S-4800 with an
96 accelerating voltage of 20 kV and EDX mode was performed using the EMAX program. The
97 sample, 1 mm thick, was pre-fractured with liquid nitrogen, attached to a cross-sectional stub
98 using carbon tape, and vacuumed to remove moisture. Sputter-coating was applied for 5
99 minutes (for non-conductive materials) at a discharge current of 10 to 20 mA to eliminate
100 surface layers or contaminants.

101 **3. Results and Discussion**

102 *3.1. Effect of amine-based compounds as devulcanizing agent during the Rubber Reclamation*

103 *Process*

104 Caprolactam and hexamethylenediamine are two compounds used in this study because
105 they contain primary and secondary amine (Mousavi et al., 2016). It would be compared to
106 Tetraethylenepentaamine (TEPA) which also contains primary and secondary amine (Jiang et
107 al., 2018). Primary and secondary amine were expected to show a high degree of
108 devulcanization and sol content, and lower crosslink density on the ground tire rubber.

109

110

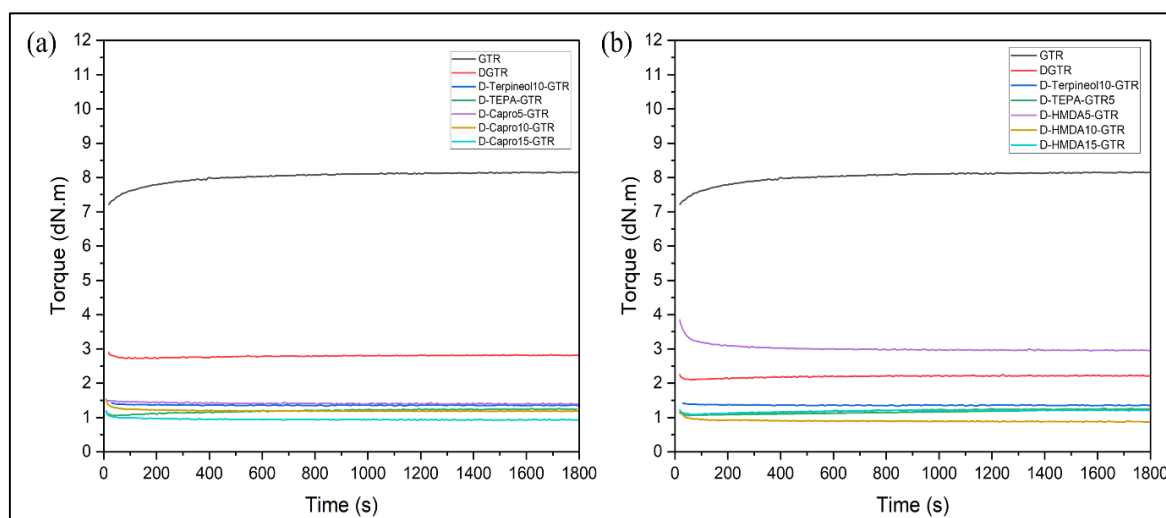
111 *3.1.1. Characteristics of Reclaimed Rubbers*

112 Increasing the amount of devulcanizing agent showed increasing the devulcanization
 113 degree and sol fraction. **Table 1**, Using (5; 10; and 15 phr) of caprolactam and
 114 hexamethylenediamine also get lower crosslink density and the torque profile. For
 115 caprolactam, it showed from 5 to 15 phr gives a higher degree of devulcanization
 116 approximately 78% than TEPA (70%). On the other hand, using hexamethylenediamine
 117 started from 10 to 15 phr gives a higher sol content approximately 8% than TEPA (3%). This,
 118 in turn, demonstrated the sol fraction's strong dependency on reclaiming agent content.
 119 During devulcanization, GTR experiences massive mechanical shearing in a lower-
 120 temperature environment, resulting in random polymer chain breakup (Zhang et al., 2018). A
 121 reduced total crosslink density is the consequence of successful devulcanization, which is
 122 often shown by a larger sol fraction and lower gel fraction. This is because the crosslinks in
 123 the rubber matrix are broken during the devulcanization process, increasing the amount of
 124 soluble polymer chains (sol fraction) and decreasing the crosslinked network (gel fraction)
 125 (Barbosa & Ambrósio, 2019).

126 **Table 1.** Sol-gel fraction, swelling, crosslink, and devulcanizing degree using caprolactam
 127 and hexamethylenediamine as a devulcanizing agent.

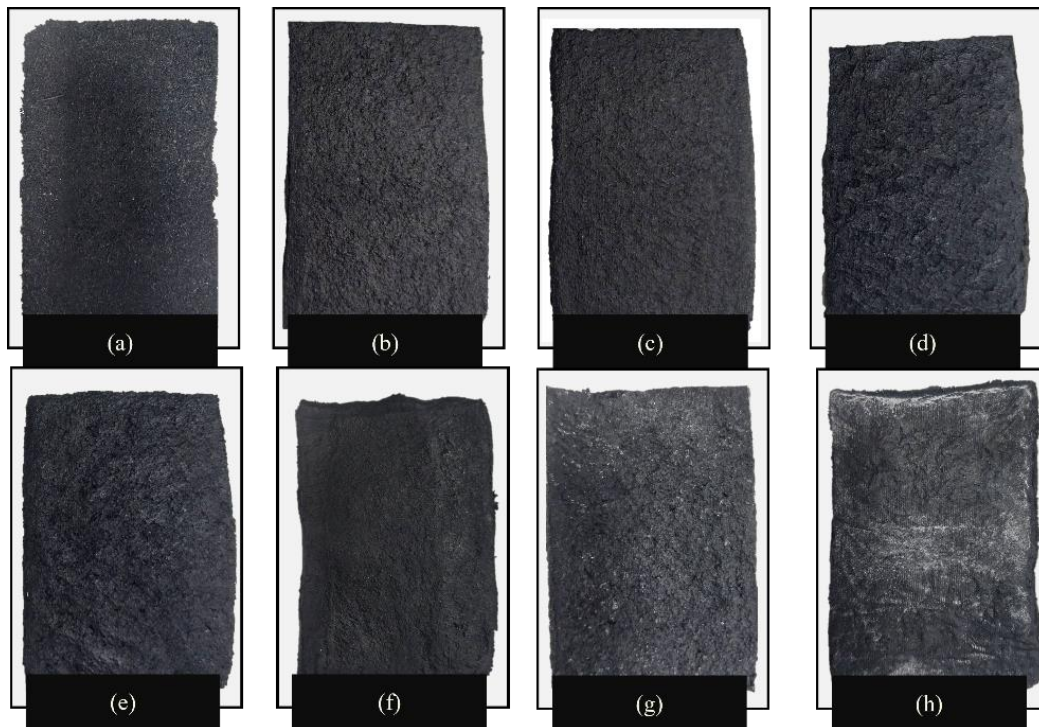
Sample code	Sol (%)	Gel (%)	Swelling (%)	CLD (10^{-4} mol/cm ³)	DD (%)
DGTR	6.8	93.2	257.9	7.9	50.9
D-Terpineol-GTR	10.6	89.4	262.8	7.3	63.8
D-TEPA-GTR	9.01	90.9	343.2	5.9	70.8
D-Capro5-GTR	14.9	85.1	304.0	5.0	68.9
D-Capro10-GTR	20.3	79.7	271.2	4.9	75.2
D-Capro15-GTR	23.6	76.4	282.0	4.4	77.6
D-HMDA5-GTR	14.4	85.6	238.7	13.2	34.5
D-HMDA10-GTR	16.9	83.1	278.9	9.2	54.1
D-HMDA15-GTR	11.8	88.2	291.6	8.4	58.0

128 At higher devulcanization degrees, torque decreases due to lower crosslink density.
129 Lower crosslink density is the result of crosslinks breaking during the devulcanization of
130 rubber. Generally, this method softens the material and enhances polymer chain mobility,
131 lowering the torque (Kim et al., 2020). This leads to more effective collisions among
132 molecules and higher devulcanization (**Figures 1a and b**) (Zhang et al., 2009). Figures 1a and
133 b show that the devulcanizing agent can briefly lower the crosslink density and get a high sol
134 fraction.



135 **Figure 1.** (a) The torque results from using different amounts of caprolactam and (b)
136 hexamethylenediamine.
137

138 **Figure 2** reveals the contrasting surfaces of GTR before and after adding
139 devulcanizing agents. Incorporating both processing oil and devulcanizing agent into the
140 GTR yields higher sol fraction than GTR, consequently reducing crosslink density. This
141 softening effect is quantified by the decrease in hardness (Shore A), from ± 40 for GTR to ± 30
142 after the addition of processing oil and devulcanizing agent. Thus, the observed relationship
143 between sol fraction and sample softness is the inverse correlation.

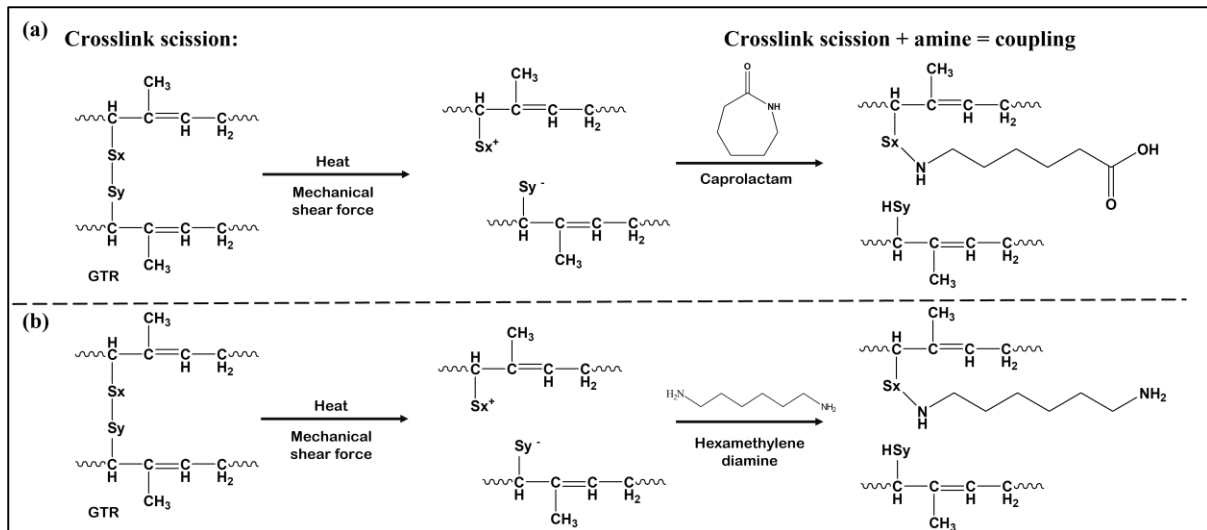


144

145 **Figure 2.** The appearance of the samples; (a) GTR; (b) DGTR; (c) D-Terpineol-GTR;
146 (d) D-TEPA-GTR; (e) D-Capro-GTR; (f) D-HMDA-GTR; (g) D-Capro-GTR (without oil);
147 (h) D-HMDA-GTR (without oil).

148 3.1.2. Mechanisms between ground tire rubber and caprolactam and hexamethylenediamine

149 When rubber networks experience high shear, the external force breaks S-S bonds,
150 creating positively charged $-S^+$ and negatively charged $-S^-$. To prevent the reattachment of
151 charged sulfur atoms, caprolactam and HMDA act as devulcanizing agents. Amine groups
152 from caprolactam and HMDA, with lone pair electrons on their N atoms, attack $-S^+$. This
153 process disrupts S-S bonds in rubber networks while preserving rubber macromolecules and
154 attaching them to amine groups in **Figure 3** (Jiang et al., 2018).

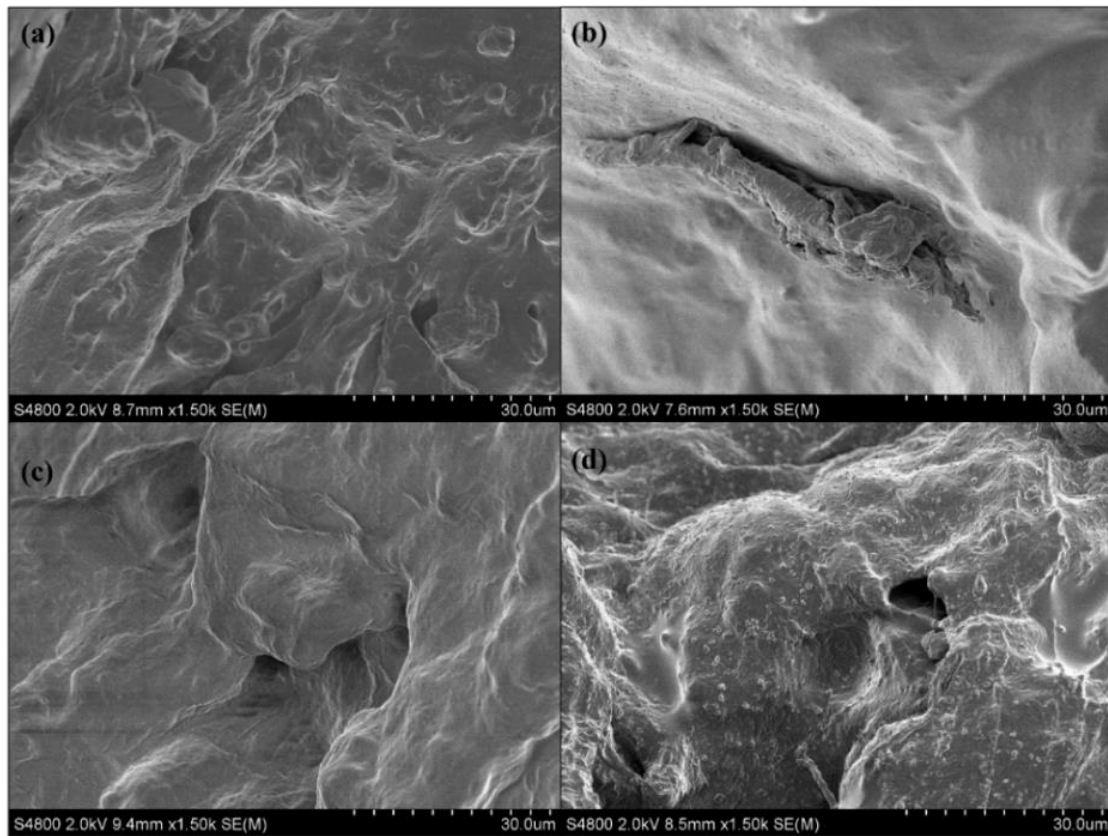


155

156 **Figure 3.** The mechanisms for (a) the mechanism between the secondary amine of
 157 caprolactam and ground tire rubber (GTR), and (b) the mechanism between
 158 hexamethylenediamine containing secondary amine with GTR.

159 **3.2. SEM-EDX**

160 The microstructure of the raw GTR exhibits a continuous and smooth appearance,
 161 suggestive of a homogeneous and cohesive material. Conversely, in **Figure 4**, the picture of
 162 devulcanized GTR (DGTR) reveals a granular structure characterized by agglomerates of
 163 rubber gels and voids. Upon the addition of caprolactam and HMDA to the GTR, these
 164 agglomerates and voids play a significant role in the devulcanization process. In particular,
 165 HMDA exhibits a propensity to crystallize at room temperature, corroborated by SEM
 166 analysis presented in **Figure 4(d)**, illustrating residual particles adhering to the GTR surface.
 167 Consequently, HMDA achieves a lower degree of devulcanization compared to caprolactam.



174

175 **Figure 4.** SEM micrograph of (a) DGTR, (b) D-TEPA-GTR, (c) D-Capro-GTR, and (d) D-
 176 HMDA-GTR using 10 phr for TEPA, caprolactam, and hexamethylenediamine in GTR.

177 However, EDX results show the remaining amount of sulfur, during the thermo-
 178 devulcanization, S-S bond scission could degrade as sulfur compounds e.g. SO₂ and H₂S as
 179 presented in **Table 2**.

180 **Table 2.** wt% from EDX of DGTR, TEPA, Caprolactam, and Hexamethylenediamine on the
 181 GTR.

Element	wt%			
	DGTR	D-TEPA-GTR	D-Capro-GTR	D-HMDA-GTR
C	77.67	50.34	42.03	52.76
N	-	16.12	38.21	18.92
O	19.11	31.05	19.63	25.95
S	3.22	2.48	0.13	2.37
Total	100			

182 This finding suggests that employing HMDA reduces sulfur degradation rather than
 183 caprolactam while preserving the main chain of the GTR. Hexamethylenediamine may also
 184 encourage more oxidation reactions since the oxidation is a part of the devulcanization

185 process which would raise the rubber's oxygen content. Hexamethylenediamine may react
186 with the rubber in a way that promotes the incorporation of ambient oxygen. This may occur
187 as a result of the more efficient exposure of oxygen-containing groups within the GTR of
188 about $\pm 26\%$ (Li & Koenig, 2005). Based on the water content in the reclaiming agents,
189 hexamethylenediamine is higher ($\pm 9\%$) than caprolactam and TEPA about similar in $\pm 2\%$.

190 **4. Conclusions**

191 In this work, increasing the concentration of amine compounds, employed as
192 devulcanizing agents, effectively enhances the degree of devulcanization and sol fraction
193 while reducing crosslink density. Starting with 5 phr of caprolactam and 10 phr of HMDA
194 yields approximately 75% and 58% devulcanization degree, respectively. EDX analysis
195 shows that caprolactam and HMDA obtained ($\pm 3\%$) of the quantified sulfur content of
196 ground tire rubber. The results provide the great potential of caprolactam and HMDA as
197 devulcanizing agents in the mechano-chemical.

198

199 **Acknowledgments:** The authors would like to express their gratitude to the National
200 Research Council of Thailand (NRCT) and the Scholarship Program for ASEAN or Non-
201 ASEAN Countries at Chulalongkorn University for supporting this research.

202

203 **Conflicts of Interest:** "The authors declare no conflict of interest."

204

205 **References**

- 206 Alonso Pastor, L. E., Nunez Carrero, K. C., Araujo-Morera, J., Hernandez Santana, M., &
207 Pastor, J. M. (2021). Setting Relationships between Structure and Devulcanization of
208 Ground Tire Rubber and Their Effect on Self-Healing Elastomers. *Polymers (Basel)*,
209 *14*(1). <https://doi.org/10.3390/polym14010011>
210 Asaro, L., Gratton, M., Seghar, S., & Ait Hocine, N. (2018). Recycling of rubber wastes by
211 devulcanization. *Resources, Conservation and Recycling*, *133*, 250-262.
212 <https://doi.org/10.1016/j.resconrec.2018.02.016>

- 213 Barbosa, R., & Ambrósio, J. D. (2019). Devulcanization of natural rubber compounds by
214 extrusion using thermoplastics and characterization of revulcanized compounds.
215 *Journal of Polymer Research*, 26(7). <https://doi.org/10.1007/s10965-019-1820-7>
- 216 Dijkhuis, K. A. J., Babu, I., Lopulissa, J. S., Noordermeer, J. W. M., & Dierkes, W. K. (2008).
217 A Mechanistic Approach to EPDM Devulcanization. *Rubber Chemistry and*
218 *Technology*, 81(2), 190-208. <https://doi.org/10.5254/1.3548204>
- 219 Guo, L., Bai, L., Zhao, J., Liu, K., Jian, X., Chai, H., Liu, F., Guo, S., Liu, G., & Liu, H.
220 (2024). Enhancing Devulcanizing Degree and Efficiency of Reclaimed Rubber by
221 Using Alcoholic Amines as the Devulcanizing Agent in Low-Temperature Mechano-
222 Chemical Process. *Polymers (Basel)*, 16(3). <https://doi.org/10.3390/polym16030395>
- 223 Jiang, C., Zhang, Y., Ma, L., Zhou, L., & He, H. (2018). Tailoring the properties of ground
224 tire rubber/high-density polyethylene blends by combining surface devulcanization
225 and in-situ grafting technology. *Materials Chemistry and Physics*, 220, 161-170.
226 <https://doi.org/10.1016/j.matchemphys.2018.08.040>
- 227 Kim, D. Y., Park, J. W., Lee, D. Y., & Seo, K. H. (2020). Correlation between the Crosslink
228 Characteristics and Mechanical Properties of Natural Rubber Compound via
229 Accelerators and Reinforcement. *Polymers (Basel)*, 12(9).
230 <https://doi.org/10.3390/polym12092020>
- 231 Li, G.-Y., & Koenig, J. L. (2005). A Review of Rubber Oxidation. *Rubber Chemistry and*
232 *Technology*, 78(3), 355-390. <https://doi.org/10.5254/1.3547889>
- 233 Mousavi, M., Pahlavan, F., Oldham, D., Abdollahi, T., & Fini, E. H. (2016). Alteration of
234 intermolecular interactions between units of asphaltene dimers exposed to an amide-
235 enriched modifier. *RSC Advances*, 6(58), 53477-53492.
236 <https://doi.org/10.1039/c6ra07506a>
- 237 Shi, J., Jiang, K., Ren, D., Zou, H., Wang, Y., Lv, X., & Zhang, L. (2012). Structure and
238 performance of reclaimed rubber obtained by different methods. *Journal of Applied*
239 *Polymer Science*, 129(3), 999-1007. <https://doi.org/10.1002/app.38727>
- 240 Sutanto, P., Laksmana, F. L., Picchioni, F., & Janssen, L. P. B. M. (2006). Modeling on the
241 kinetics of an EPDM devulcanization in an internal batch mixer using an amine as the
242 devulcanizing agent. *Chemical Engineering Science*, 61(19), 6442-6453.
243 <https://doi.org/10.1016/j.ces.2006.05.024>
- 244 Thaicharoen, P., Thamyongkit, P., & Poompradub, S. (2010). Thiosalicylic acid as a
245 devulcanizing agent for mechano-chemical devulcanization. *Korean Journal of*
246 *Chemical Engineering*, 27(4), 1177-1183. <https://doi.org/10.1007/s11814-010-0168-9>
- 247 van, D., Jacobus, W. M. N., Miriam, A. L. V., & Leen, V. D. D. (2003). US2003013776.
- 248 Wang, W., Hao, K., Guo, X., Liu, F., Xu, Y., Guo, S., Bai, L., Liu, G., Qu, L., Liu, M., Guo,
249 L., & Liu, H. (2023). Mechano-chemical rubber reclamation using aminolysis
250 products of waste flexible polyurethane foams as the devulcanizing agent. *Journal of*
251 *Cleaner Production*, 384. <https://doi.org/10.1016/j.jclepro.2022.135421>
- 252 Zhang, X., Lu, C., & Liang, M. (2009). Properties of natural rubber vulcanizates containing
253 mechanochemically devulcanized ground tire rubber. *Journal of Polymer Research*,
254 16(4), 411-419. <https://doi.org/10.1007/s10965-008-9243-x>
- 255 Zhang, X., Saha, P., Cao, L., Li, H., & Kim, J. (2018). Devulcanization of waste rubber
256 powder using thiobisphenols as novel reclaiming agent. *Waste Manag*, 78, 980-991.
257 <https://doi.org/10.1016/j.wasman.2018.07.016>

Proceedings

1 Effect of Epoxidation Degree on Self-healing Epoxidized Natural Rubber Properties: 2 Cure Characteristics, Mechanical and Abrasion resistance

3 Piyawadee Luangchuang¹, Yeampon Nakaramontri^{1*}

4 ¹Sustainable Polymer & Innovative Composite Materials Research Group, Department of
5 Chemistry, Faculty of Science, King Mongkut's University of Technology Thonburi, Bangkok
6 10140, Thailand

7 *Corresponding author: Yeampon Nakaramontri; Tel.: 0828329854

8 **Abstract:** The present study investigates the effects of two different epoxidation percentages of
9 epoxidized natural rubber (ENR) at 25 (ENR25) and 50 (ENR50) mol% on the cure
10 characteristics, mechanical properties, and self-healability regarding to the healing temperature
11 and time. To achieve the optimized self-healing propagation, ENR was modified with butyl
12 imidazole (IM) and carbon black (CB) to enhance the composites properties. It was observed
13 that the ENR25 and CB of 45 phr had effectively improved the cure properties, in terms of
14 scorch time, cure time and the estimated crosslink density. For the healed composites, this M-
15 ENR25-N45 showed also superior reproducibility on tensile properties owing to the presence
16 of ionic linkages among polarity on ENR and IM molecules. Thus, as a results, the composites
17 can be proposed for future tire and healable products under cost-effectiveness and simply on
18 preparation procedure.

19 **Keywords:** Epoxidized Natural Rubber (ENR); Imidazole; Self-healability.

20 1. Introduction

21
22 Natural rubber (NR) has been recognized as a versatile elastomer with various mechanical
23 applications owing to its desirable mechanical properties [1]. However, its susceptibility to
24 damage, such as cracks and cuts, has prompted significant investigation into self-healing
25 materials to extend its life expectancy and durability. One promising avenue involves the
26 incorporation of healing agents, such as imidazole (IM), into epoxidized natural rubber (ENR)
27 composites filled with carbon black (CB).

28 Hence, rubber composites filled with carbon-based particles were found to be an
29 appealing choice towards the improvement of new materials suitable for tire applications,
30 especially inner liner, and tire treads. Recently, self-healing rubber has been proposed with
31 the movement of positive and negative charges across the cutting interfaces. Moreover, it has
32 been found that a combination of conductive filler in the composite significantly improves the
33 healing behavior of the composites [2,3]. Consideration of self-healing composites for
34 extending the possibilities in tire applications, it is a promising and challenging area of
35 research, aiming to improve the electrical conductivity and durability.

36 Therefore, a self-healing ENR25 and ENR50 modified with butyl imidazole (IM)the
37 ENR filled with CB. The work aims to provide important insights into the design and
38 optimization of self-healing epoxide natural rubber composites with superior cure time,
39 mechanical and abrasion resistance. The goal is to promote the usage of such composites for
40 tire applications, and it is a promising and challenging area of research.

42 **2. Experimental**

43 **2.1 Materials**

44 Epoxidized natural rubbers (ENR) with 25 and 50 mol% of the epoxirane ring on the
45 ENR mainchains were purchased from Muang Mai Guttrie Public Company Limited (Surat
46 Thani, Thailand). In addition, conductive carbon black (CCB) grade Vulcan XC72 were
47 purchased from Cabot Corporation (Pampa, TX, USA). The 1-butylimidazole (IM) was
48 received from Merck KGaA (Darmstadt, Germany). Stearic acid was procured from Imperial
49 Chemical Co., Ltd. (Pathum Thani, Thailand). Zinc oxide (ZnO) and sulfur were manufactured
50 by Global Chemical Co., Ltd. (Samutprakarn, Thailand) and Ajax Chemical Co., Ltd.
51 (Samutprakarn, Thailand), respectively. N-Cyclohexylbenzothiazol-2-sulphenamide
52 (CBS) was purchased from Bos ofticon Limited Partnership (Songkhla, Thailand).

53 **2.2 Preparation of composites**

54 Preparation procedures for the ENR25 and ENR50 composites were carried out
55 according to the formulation shown in Table 1. Initially, the modification of ENR using an
56 internal mixer at 40°C and a rotor speed of 60 rpm was performed. ENR25 and ENR50 were
57 masticated for 2 minutes before adding the activators, with mixing continuing for an
58 additional 2 minutes. The CB was then added and continued mixing for another 4 minutes. IM
59 was introduced into the compound, following with the curatives and the mixing was fixed for
60 the total mixing time of 14 minutes. The compound was sheeted at 160°C using compression
61 molding to obtain the 2 mm crosslinked composites following the rheometer testing. It is
62 noted that the modified ENR25 and ENR50 composites with IM and CB were designated
63 using the code “M-ENR25-N45 and M-ENR50-N45”.

64 **2.3 Cure characterization**

65 Cure characteristics of composites with CB were determined using a moving die
66 rheometer (MDR, Monsanto Co., Ltd., Findlay, OH, USA) following the ASTM D5289. The
67 measurements were performed at a fixed oscillating frequency of 1.66 Hz with 1 arc degree
68 amplitude at 160°C. The T_{c90} is the cure time of the sample and $M_H - M_L$ is the difference
69 between maximal and minimal torques as a function of time.

70 **2.4 Mechanical Properties**

71 Mechanical properties, based on tensile testing following ISO 37 (type 2) were
72 measured using a tensile testing machine (model 3365, Instron® Inc., Massachusetts, USA).
73 To measure self-healing ability, dumbbell-shaped samples were also cut using a sharp razor
74 blade before being pressed into the mold and heated at 160°C for 15 minutes without applying
75 any pressure. The healed samples were measured the mechanical properties under the tensile
76 testing mode as the same condition of the unhealed cases. The healing efficiency (X^*), which
77 is the ratio of the obtained values before (X') and after (X'') healing conditioning, was
78 calculated using Equation (1):

79 **2.5 Abrasion Resistance**

80 Abrasion testing of the composites was conducted to indicate their surface detachment
81 resistance while performing in the Taber tester (Model GT-7012-T, GoTech, Taichung,
82 Taiwan), using a maximum of 5 specimens for each formulation following the ASTM D4060.
83 The samples, approximately 110 mm in diameter with 2 mm of thickness, were polished
84 under a 72 rpm rolling speed for 1000 cycles, and the wear index (WI) was calculated
85 following Equation (2):
86

87 **3. Results and Discussion**

88 **3.1 Cure Characterization**

89 Figure 1 shows the cure curves of M-ENR25-N45 and M-ENR50-N45 by reinforcing
90 with the fixed CB and IM modifying agent. It is clearly seen that both curves had shown the
91 reversion behavior due to the poor thermal stability of the ENR regarding thermo-oxidative
92 degradation. In addition, Table 2 summarizes the cure properties of both composites, and it was
93 found that the composites showed increase of the cure time (T_{c90}) with increasing the epoxide
94 group. This can be attributed to the ENR25 had a higher amount of double bonds compared to
95 ENR50 rubber, which leads to the vulcanization reaction occurring faster. In addition, this is
96 also due to the incorporation of CB into the ENR matrix. This filler enhances the strength and
97 heat conductivity, allowing the rubber to undergo vulcanization reaction faster as well. It is
98 noted that the dispersion and distribution of CB throughout the ENR depend on ENR polarity.
99 With higher polarity, ENR might cause self-interaction, preventing interaction between ENR
100 and CB surfaces. Thus, the dispersion of CB inside the ENR matrix can be reduced with a
101 higher level of the epoxide ring. Therefore, with poor dispersion, thermal expansion through
102 the CB network is limited, resulting in an increased cure time. In addition, the M_H-M_L value of
103 ENR25 rubber surpasses that of ENR50 rubber due to its higher double bond content, leading
104 to increased cross-linking. Additionally, the inclusion of fillers further elevates the M_H-M_L
105 value. This enhancement is attributed to ENR25 rubber's superior interaction with carbon
106 black, stemming from their similar polarities [4].

107 **3.2 Mechanical properties**

108 Mechanical properties in terms of tensile strength, elongation at break and 100%
109 modulus of ENR composites are demonstrated in Figure 2 and summarized in Table 3. In figure
110 2(a), it was found that in the case of M-ENR25-N45, the tensile strength, elongation at break,
111 and 100% modulus are higher than those of M-ENR50-N45. This is due to ENR25 rubber
112 exhibiting higher crosslink density and better strain-induced crystallization (SIC) behavior
113 compared to ENR50 rubber [5,6]. Additionally, the inclusion of molecularly modified (IM)
114 agents results in grafting of IM molecules onto the rubber chain, inducing attractive forces
115 between the chains, as seen the proposed reaction in Figure 5. Reaction shows reaction of IM
116 molecules and ENR molecular chains which can be generated during mixing inside the internal
117 mixer. This ENR modification causes cation and anion on ENR mainchain which can be
118 reversible after breakage. This may lead to rapid alignment of positively and negatively charged
119 rubber chains during stretching, resulting in enhanced strain-induced crystallization behavior
120 and increased difficulty in slippage, thus resulting in higher tensile strength, elongation at
121 break, and 100% modulus compared to ENR50 rubber [7].

122 The mechanical properties of reprocessed or recrosslinked composite rubber can be
123 indicated in Figure 2(b) and Table 3. Results show a decrease in tensile strength, elongation at
124 break, and 100% modulus compared to both M-ENR25-N45 and M-ENR50-N45 composites
125 before healing (Figure 2(a)). This decline is attributed to different rate of the self healability
126 of the ionic crosslinking inside both ENR25 and ENR50. Also, with the self-attraction among
127 the functional group on ENR mainchain, lower epoxirane ring might perform better healing
128 rate [7].

129 Upon analysis of the healing efficiency of composite rubber in Figure 3 and Table 4,
130 results show performance of self repairing in both ENR25 and ENR50 rubbers after breakage
131 [8]. This self recovering is attributed to efficient chemical bond formation through alkylation
132 reactions and the isolation of ionic cluster groups, which align rubber chains and improve
133 healing. Furthermore, M-ENR50-45 rubber exhibits superior self-healing compared to M-
134 ENR25-N45, attributed to IM molecule grafting, enhancing attractive forces between rubber
135 chains, and aiding self-healing surface fusion. Additionally, filler agent improvements in

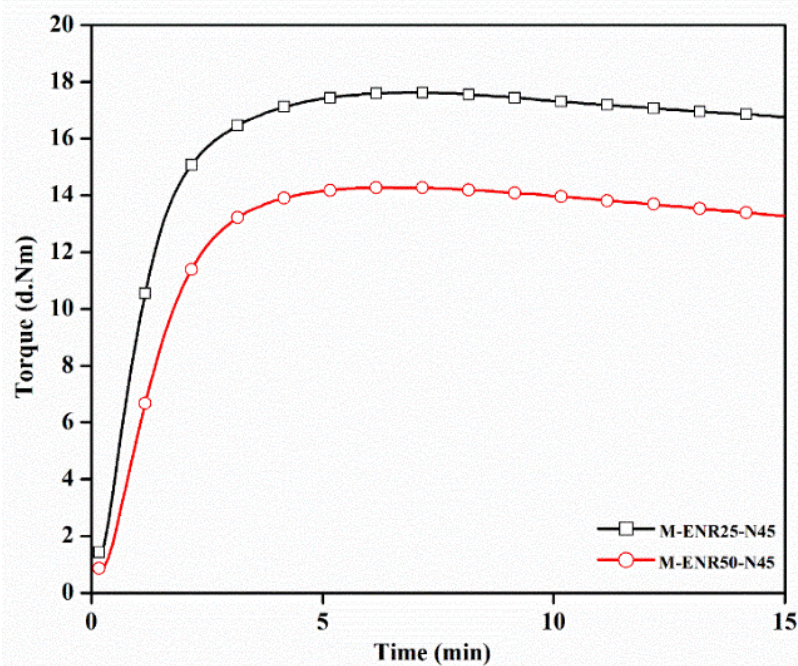
136 electrical conductivity and heat conduction enhance chain movement, further improving self-
137 healing efficiency [6].

138 3.3 Abrasion resistance

139 Figure 4 shows the Wear index of the composite, where a low wear index indicates
140 excellent wear resistance. It can be observed that the M-ENR25-N45 exhibits the lowest wear
141 index compared to the M-ENR50-N45. This result is attributed to the higher crosslink density
142 of M-ENR25 rubber, which is achieved by adding a modifying agent that adjusts the charge on
143 the rubber molecules. At this stage, grafting IM onto ENR molecular chains can be initiated by
144 the reaction shown in Figure 5, which occurs at the hydroxyl groups due to the epoxirane ring
145 opening. As the hydroxyl groups increase, physical and chemical self-interactions among the
146 ENR chains also increase, which hinders the reaction between IM and ENR. This means that,
147 with a decrease in polarity on the rubber main chain, higher crosslinking propagation can occur
148 during the mixing and compressing processes. Consequently, this facilitates easier movement
149 of the molecules and enhances the self-coordination efficiency of the rubber.

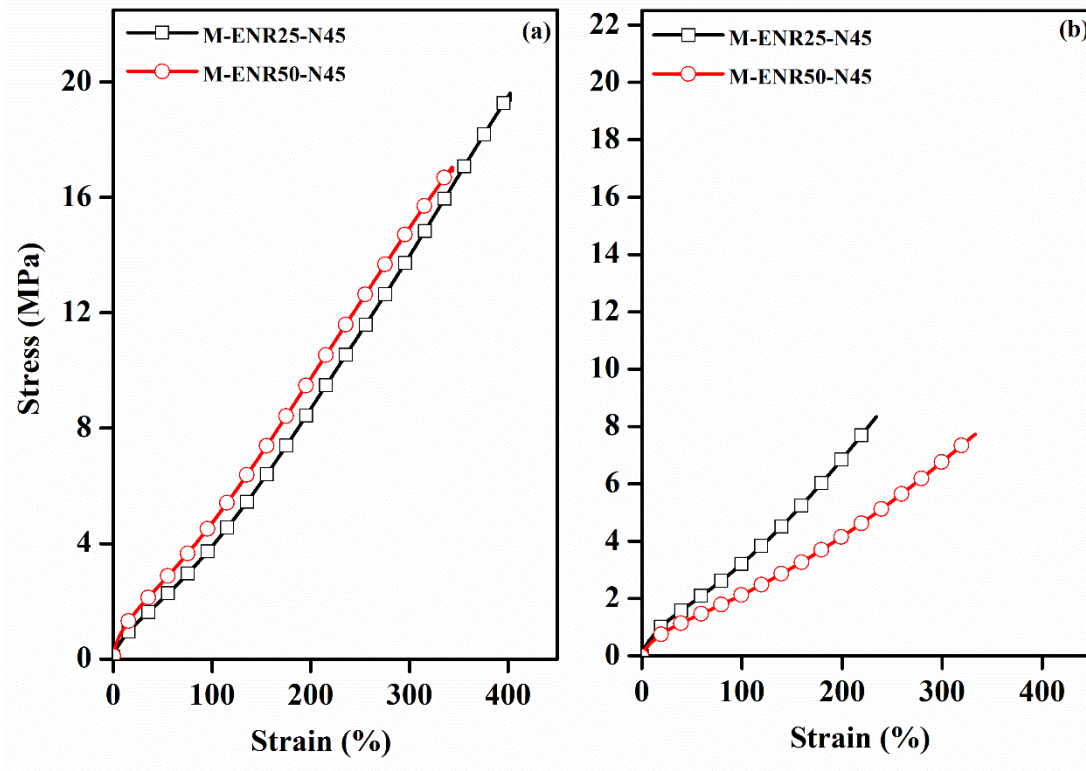
150

151 3.4. Figures, Tables and Schemes



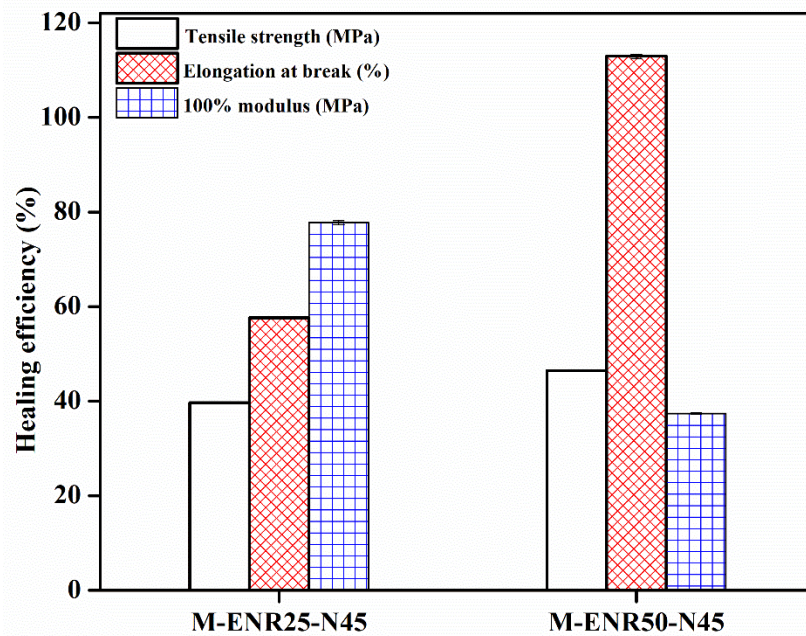
152

153 **Figure 1.** Cure characteristics curves of M-ENR25-N45 and M-ENR50-N45.



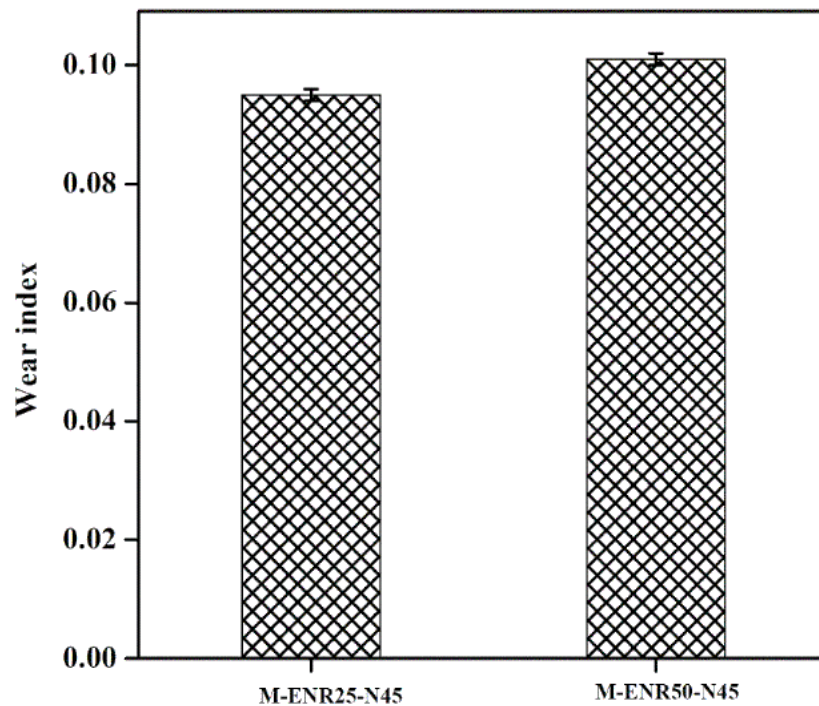
154

155 **Figure 2.** Stress-Strain curves of M-ENR25-N45 and M-ENR50-N45 before (a) and after
 156 healing (b).



157

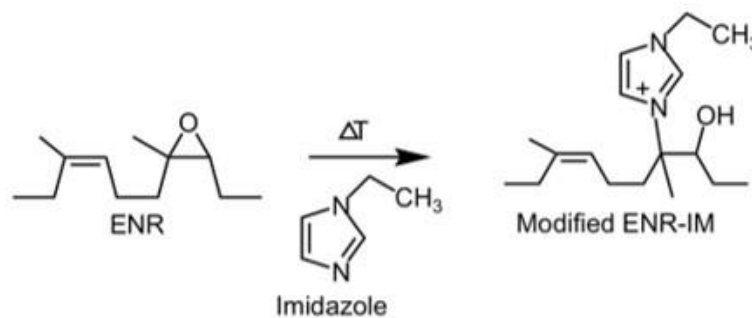
158 **Figure 3.** Healing efficiency of M-ENR25-N45 and M-ENR50-N45 based on tensile
 159 properties.
 160



161

162

Figure 4. Wear index of M-ENR25-N45 and M-ENR50-N45.



163

164

165

Figure 5. Proposed reaction propagation that occurred during mixing and compressing processes by crosslinking with ENR molecules and IM.

166

167

168

Table 1. Formulation of ENR25 and ENR50 composites.

Ingredients	Chemical roles	Contents (phr)	
		Formula 1	Formula 2
ENR25	Rubber matrix	100	-
ENR50	Rubber matrix		100
IM	Modify agent	5	5
CCB	Filler	45	45
ZnO	Activator	5	5
Stearic acid	Activator	2	2
Accelerator	Accelerator	1.7	1.7
Sulfur	Vulcanizing agent	1.4	1.4

169

170

171
172

Table 2. Cure characteristics of modified ENR25-N45 and ENR50-N45.

Samples	T _{c90} (min)	M _H (d.Nm)	M _L (d.Nm)	M _H -M _L (d.Nm)
M-ENR25-N45	2.74	17.64	1.42	16.22
M-ENR50-N45	2.92	14.29	0.83	13.46

173
174
175
176

Table 3. Tensile strength, elongation at break and 100% modulus of composites before and after self-healing propagation.

Samples	Tensile strength (MPa)		Elongation at break (%)		100% modulus (MPa)	
	Before healing	After healing	Before healing	After healing	Before healing	After healing
M-ENR25-N45	19.61±0.04	8.26±0.03	402±0.32	232±0.09	3.91±0.10	3.04±0.09
M-ENR50-N45	17.05±0.03	7.75±0.03	343±0.25	388±0.28	4.71±0.12	1.76±0.06

177
178

Table 4. Healing efficiency based on tensile strength, elongation at break and 100% modulus.

Samples	Healing efficiency (%)		
	Tensile strength (MPa)	Elongation at break (%)	100% modulus (MPa)
M-ENR25-N45	42.12±0.12	57.61±0.23	77.75±0.40
M-ENR50-N45	45.45±0.19	112.97±0.45	37.37±0.13

179
180

3.5. Formatting of Mathematical Components

$$X^*(\%) = \frac{X'}{X} \times 100 \quad (1)$$

$$WI = \frac{(W_x - W_y)}{\text{Specific gravity}} \quad (2)$$

183
184

W_x is the weight before loss mass and W_y is the weight after loss mass.

4. Conclusion

The self-healing composites based on modified M-ENR25-N45 and M-ENR50-N45 formulations were studied. The results showed that the M-ENR25-N45 exhibits superior reproducibility in tensile properties due to the presence of ionic linkages among ENR and IM molecules regarding the lowering of the self-crosslinking among the ENR molecular chain owing to high level of polarity of the rubber mainchains. **Consequently, these composites are suggested for tire and healable product applications due to their simple preparation procedure.**

Author Contributions: P.L.: Conceptualization, Methodology, Validation, Formal analysis, Writing—original draft preparation, T.S.: Conceptualization, Methodology, Validation, Formal analysis, Y.N.: Visualization, Supervision, Formal analysis, Writing—review and editing, Funding acquisition. All authors have read and agreed to the published version of the manuscript.

Funding: This research was funded by the Ministry of Higher Education, Science, Research, and Innovation, grant number RGNS 64-100, and the National Science, Research, and Innovation Fund, grant number B01F640031.

200 **Acknowledgments:** This work (Grant No. RGNS 64-100) was supported by the Office of the
201 Permanent Secretary, Ministry of Higher Education, Science, Research and Innovation (OPS
202 MHESI), Thailand Science Research and Innovation (TSRI). Additionally, the National
203 Science, Research, and Innovation Fund (NSRF) via the Program Management Unit for
204 Human Resources and Institutional Development, Research and Innovation [grant number
205 B01F640031] was acknowledged.

206 **Conflicts of Interest:** “The authors declare no conflict of interest.”

207 References

- 208 1. Wu, X.; Lu, C.; Zhang, X.; Zhou, Z. Conductive natural rubber/carbon Black
209 nanocomposites via cellulose nanowhisker templated assembly: Tailored hierarchical
210 structure leading to synergistic property enhancements. *J. Mater. Chem. A* **2015**, *25*,
211 13317–13323.
- 212 2. Das, A.; Sallat, A.; Böhme, F.; Suckow, M.; Basu, D.; Wießner, S.; Heinrich, G. Ionic
213 modification turns commercial rubber into a self-healing material. *ACS Appl. Mater.*
214 *Interfaces* **2015**, *7*, 20623–20630.
- 215 3. Le, H.H.; Hait, S.; Das, A.; Wiessner, S.; Stoeckelhuber, S.; Boehme, K.W.F. Radusch,
216 H. Self-healing properties of carbon nanotube filled natural rubber/bromobutyl rubber
217 blend. *Express Polym. Lett.* **2017**, *11*, 230–242.
- 218 4. Hanafi Ismail, B.T Poh. Cure and tear properties of ENR 25/SMR L and ENR 50/SMR
219 L blends, *Eur Polym J.* 2000, 36(11), 2403–2408.
- 220 5. Toki, S. The effect of strain-induced crystallization (SIC) on the physical properties of
221 natural rubber (NR). In *Chemistry, Manufacture and Applications of Natural Rubber.*
222 2014, (pp. 135-167).
- 223 6. Pire, M., Norvez, S., Iliopoulos, I., Le Rossignol, B., & Leibler, L. Epoxidized natural
224 rubber/dicarboxylic acid self-vulcanized blends. *Polymer.* 2010, 51(25), 5903-5909.
- 225 7. Luangchuang, P.; Sornanankul, T.; Nakaramontri, Y. Effects of modifying agent and
226 conductive hybrid filler on butyl rubber properties: mechanical, thermo-mechanical,
227 dynamical and re-crosslinking Properties. *Polym.* 2023, 15(19), 4023.
- 228 8. Suckow, M., Mordvinkin, A., Roy, M., Singha, N.K., Heinrich, G., Voit, B.,
229 Saalwächter, K. and Böhme, F, 2018, Tuning the properties and self-healing behavior
230 of ionically modified poly(isobutylene-co-isoprene), *Macromolecules*, Vol.51, pp.468-
231 479.

232

Proceedings

1 **Life Cycle Assessment of Composite Based on ENR/Wet Blue Leather**

2 **Worachai Techo¹, Laksamon Raksaksri^{1,2*}**

3 ¹ School of Polymer Engineering, Institute of Engineering, Suranaree University of Technology, Nakhon
4 Ratchasima 30000, Thailand.

5 ² Research Center for Biocomposite Materials for Medical Industry and Agricultural and Food Industry,
6 Suranaree University of Technology, Nakhon Ratchasima 30000, Thailand.

7 *Correspondence: Laksamon@g.sut.ac.th; Tel: +66954367746

8 Life Cycle Assessment of Composite Based on ENR/Wet Blue Leather, Breakout Foyer of Koh Tachai
9 and Koh Panyi, 28 February 2024.

10 **Abstract:** Wet blue leather scrap from the leather industry is possible to end up in landfills. These have
11 an impact on the environment. The objective of this study is to assess and compare routes between
12 landfills and recycled materials. Environmental impacts include acidification potential, climate change,
13 depletion of abiotic resources - elements, ultimate reserves, depletion of abiotic resources - fossil fuels,
14 eutrophication, freshwater aquatic ecotoxicity, human toxicity, marine aquatic ecotoxicity, ozone layer
15 depletion, photochemical oxidation, terrestrial ecotoxicity. OpenLCA software version 2.1.1 and impact
16 assessment method CML-baseline version 4.4. were used for life cycle assessment in this study. The
17 landfill route shows a higher risk number than the recycled materials route in almost every aspect.
18 Especially freshwater aquatic ecotoxicity, human toxicity, and terrestrial ecotoxicity.

19

20 **Keywords:** Life cycle assessment; recycle; epoxidized natural rubber; composite; leather; wet
21 blue leather.

22

23 **1. Introduction**

24 Environmental problems are now a global concern. It is estimated that there are
25 approximately 1 billion cattle globally, of which about 300 million are slaughtered each year.
26 Of these, 55% of the hides are turned into leather, while 45% go to waste. This means that 135
27 million hides per year end up in landfills. Chrome metal is widely used as a tanning agent in

28 leather production. This chemical substance is known to be carcinogenic and causes
29 environmental pollution.

30 *1.1. Life cycle assessment*

31 Ulya *et al.*² studied the life cycle assessment of cow-tanned leather products. The study
32 aims to estimate the environmental impact of cow-tanned leather. In production in Indonesia,
33 the life cycle assessment (LCA) method used was a gate-to-gate perspective to obtain the
34 environmental impact at each stage of cow leather production. The leather tanning industry
35 produces liquid waste and solid waste in its production. As a result, the leather tanning process
36 in Indonesia showed several impact categories, in which marine aquatic ecotoxicity of tanning
37 was the highest concern at the value of 38800 Kg 1,4-dichlorobenzene eq.

38 *1.2. Composite*

39 A composite is something made up of multiple distinct parts or elements. In various
40 contexts, such as materials science, it denotes a material composed of two or more different
41 substances that retain their individual characteristics while contributing to improved
42 performance properties, such as strength or durability, when combined. Li *et al.*³ found that the
43 effect of triethoxyvinylsilane-modified leather collagen fibers (M-LCF) improves the
44 mechanical properties of the composite. The tensile strength, elongation, and fracture
45 toughness of the NR/M-LCF with 5% modified collagen fibers reached 18.76 MPa, 740%, and
46 54.09 MJ·m⁻³, respectively. The composite has higher tensile strength, elongation, and fracture
47 toughness than natural rubber. Laurentia *et al.*⁴ produced a new biodegradable composite
48 material using post-consumption thermoplastic polyurethane waste (WTPU) compounded with
49 post-consumption finished leather waste (WL). using a double-screw extruder at 1% by weight
50 of polyethylene grafted with maleic anhydride and up to 20% by weight of fiber content. The
51 effect of WTPU showed the reduction of elongation at break, elasticity, and tear strength but
52 an increase in hardness. there is increased hardness. Makes the composite more rigid. However,
53 the tear resistance is more than twofold reduced compared to WTPU. Meyer *et al.*⁵ compared
54 the structure and technical performance of shoe upper leather with nine alternative materials,

55 the coarse fiber bundle mesh layer has the function of high mechanical resistance, tensile
56 strength, and tear strength.

57 Stefaniak *et al.*⁶ showed that phytochemicals from catechin hydrate, eugenol, and flavone
58 could be used as a natural antioxidant for epoxidized natural rubber (ENR) and poly (lactic
59 acid) (PLA) green composites. Surana *et al.*⁷ found that adding leather particles 15 wt%
60 increased compressive toughness by 29% of leather/HDPE-epoxy blended composite. Fracture
61 surface analysis showed that the aggregation of small leather particles size 800 µm caused a
62 change in the failure of epoxy from brittle to tough.

63 1.3. Waste management

64 Currently, there is an increased demand for vehicles. Resulting in the use of more tires in
65 production and use of vehicles. This directly results in more tire waste, which is waste that is
66 difficult to recycle. Meng *et al.*⁸ studied rubber waste management in China and reported that
67 47.07% of waste is truck tire waste, therefore, switching to a more integrated mix of clean
68 energy could be a good way to reduce the environmental impact of rubber waste. There are
69 ways to recycle rubber waste as follows: Reclaimed rubber production (RRP), rubber powder
70 production (RPP), pyrolysis (PRS), tire retreading (TR), and prototype utilization (PU). Fela *et*
71 *al.*⁹ proposed the leather waste substitution of hard coal for energy recovery. Wan *et al.*¹⁰
72 showed that the presence of microplastics in landfill waste in the bottom soil varied from 590
73 to 103080 items/kg and from 570 to 14200 items/kg, respectively.

74 This study aims to use leather waste, wet blue leather mixed with epoxidized natural rubber
75 (ENR) to make an artificial leather composite. Therefore, the life cycle impacts of wet blue
76 leather discarded in the landfill were assessed and compared to the composites. To analyze the
77 impacts including acidification potential (average Europe), climate change (global warming
78 potential 100-year), depletion of abiotic resources (elements, ultimate reserves), depletion of
79 abiotic resources (fossil fuels), eutrophication (generic), freshwater aquatic ecotoxicity, human
80 toxicity, marine aquatic ecotoxicity, ozone layer depletion (steady state), photochemical
81 oxidation (high oxides of nitrogen, NO_x), terrestrial ecotoxicity. The purpose of this work is
82 mainly to prove that composite could be an optional project to replace landfill route.

83 2. Experimental

84 This experiment is performed by openLCA software version 2.1.1. The method used is
 85 CML-baseline version 4.4 and database used is LCIA method pack for openLCA nexus by
 86 Cristina Rodríguez, Claudia di noi, Michael Srocka, Andreas Ciroth is licensed under a creative
 87 commons attribution-sharealike 4.0 international license. Based on work on www.openlca.org
 88 and various impact assessment models. Permissions beyond the scope of this license may be
 89 available at www.greendelta.com, database name used in this experiment is
 90 *openlca_lcia_methods_1_5_7*.

91 2.1. Material flow

92 The experiment starts with defining various components in the material flow format,
 93 creating the flow as shown in table 1.

94 **Table 1.** Material flows process.

Flow name	Flow type	Reference flow property
Soaking	Product	Mass
Liming	Product	Mass
Fleshing	Product	Mass
Deliming	Product	Mass
Bating	Product	Mass
Pickling	Product	Mass
Chrome Tanning	Product	Mass
Neutralization	Product	Mass
Washing I	Product	Mass
Splitting	Product	Mass
Shaving	Product	Mass
Landfill	Product	Mass
Washing II	Product	Mass
Drying	Product	Mass
Compounding	Product	Mass
Two Roll Mill	Product	Mass
Compression molding	Product	Mass

95

96 2.2. Process

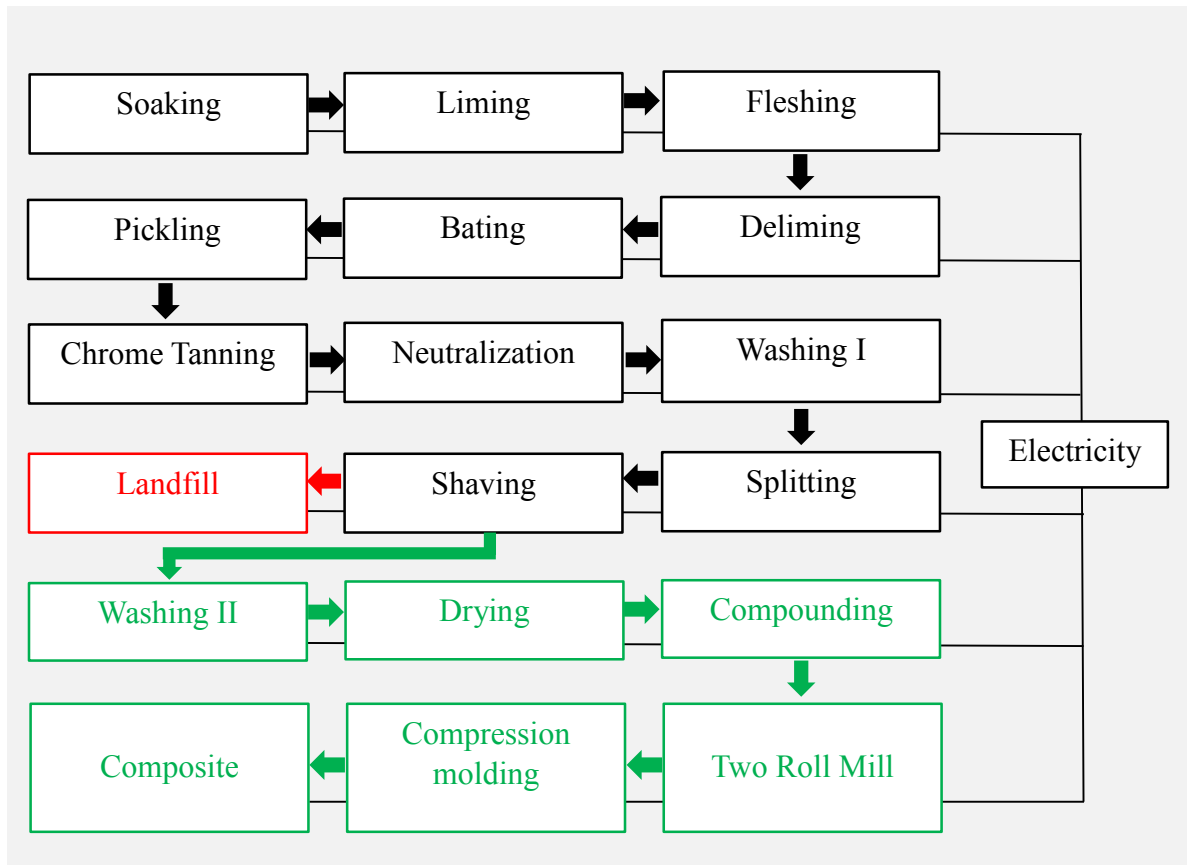
97 The leather production is the main source of wet blue leather waste. The experimental aim
 98 is to compare two main routes. The former is “landfill” and the latter “composite”. In each
 99 process, an input/output will be specified which consists of raw materials, machinery electricity
 100 in each step, and components as shown in Table 2.

101 **Table 2.** Process input and output.

Step	Process	Input flow	Amount	Unit	Output flow	Amount	Unit
1	Soaking	Electricity	0.92	kWh	Cowhide, Soaking	138.30	g
		Raw cowhide	138.30	g			
2	Liming	Cowhide, Soaking	138.30	g	Cowhide, Liming	138.30	g
		Electricity	1.54	kWh			
		Glucose	0.30	g			
3	Fleshing	Cowhide, Liming	138.30	g	Cowhide, Fleshing	135.30	g
					Waste (solid)	276.10	g
4	Deliming	Cowhide, Fleshing	676.20	g	Cowhide, Deliming	676.20	g
		Electricity	1.64	kWh			
		Protease enzyme	0.22	g			
5	Bating	Cowhide, Deliming	676.20	g	Cowhide, Bating	676.20	g
		Electricity	1.64	kWh			
6	Pickling	Cowhide, Bating	676.20	g	Cowhide, Pickling	676.20	g
		Electricity	3.43	kWh			
7	Chrome Tanning	Cowhide, Pickling	676.20	g	Cowhide, Wet Blue	298.20	g
		Electricity	7.84	kWh			
8	Neutralization	Cowhide, Wet Blue	298.20	g	Cowhide, Neutralization	298.20	g
		Electricity	0.22	kWh			
9	Washing I	Cowhide, Neutralization	298.20	g	Cowhide, Washing	280.20	g
		Electricity	0.19	kWh			
10	Splitting	Cowhide, Washing	298.20	g	Cowhide, by-product	149.20	g
		Electricity	1.01	kWh	Cowhide, Splitting	149.20	g
11	Shaving	Cowhide, Splitting	149.20	g	Cowhide, Shaving	149.20	g
		Electricity	0.26	kWh			
Route 1	Landfill	Cowhide, Shaving	400.00	g	Landfill of textiles	400.00	g
		Cowhide, Shaving	150.00	g			
	Drying	Electricity	1.00	kWh	Wet Blue Leather (Pass oven)	150.00	g
		Wet Blue Leather (Pass washing)	150.00	g			
	Compounding	Wet Blue Leather (Pass oven)	150.00	g	Compound (Pass compounding)	400.00	g
		Epoxidized natural rubber (ENR)	250.00	g			
Route 2	Two Roll Mill	Electricity	1.00	kWh	Compound (Pass two roll mill)	400.00	g
		Compound (Pass compounding)	400.00	g			
	Compression molding	Electricity	1.00	kWh	Composite based on ENR/Wet blue leather	400.00	g
		Compound (Pass two roll mill)	400.00	g			
		Electricity	1.00	kWh			

103 2.3. Product systems

104 Create a product system of landfill route and composite route by linked various processes
 105 as shown in figure 1.



106

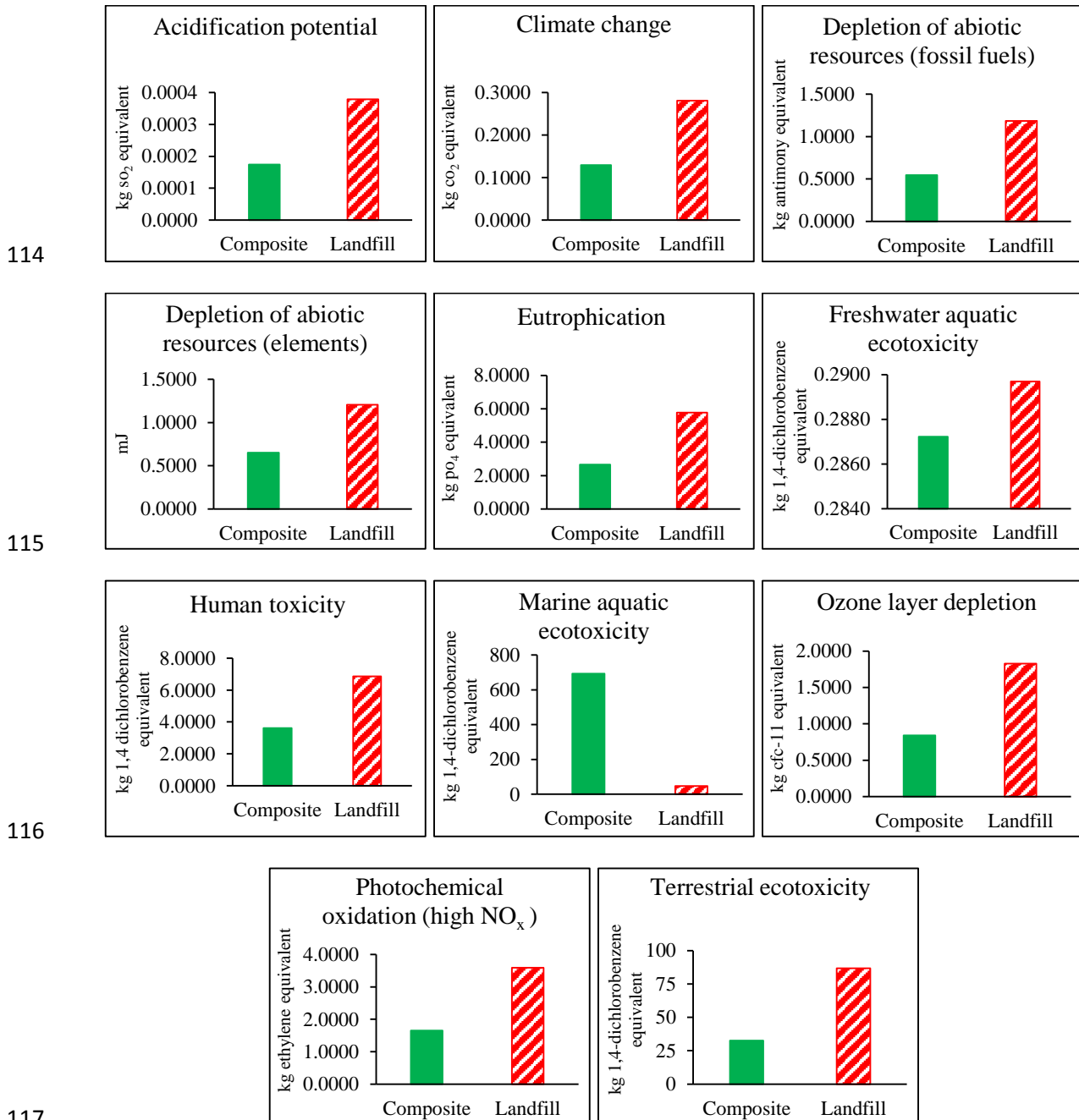
107 **Figure 1.** Product systems.

108 2.4. Project

109 It is an environmental impact comparison step between the product system of the landfill
 110 route and composite route using the impact assessment method CML-baseline version 4.4. to
 111 display impact categories.

112 **3. Results and Discussion**

113 *3.1. Impact on environment*



118 **Figure 2.** Impact categories comparison.

119 **Table 3.** Life cycle assessment of composite and landfill routes.

Impact Categories	Composite	Landfill	Unit
Acidification potential (average Europe)	0.0002	0.0004	kg SO ₂ equivalent
Climate change (Global Warming Potential 100-year)	0.1295	0.2808	kg CO ₂ equivalent
Depletion of abiotic resources (elements, ultimate reserves)	0.6511×10^{-5}	1.2054×10^{-5}	kg antimony equivalent
Depletion of abiotic resources (fossil fuels)	0.5454	1.1852	mJ
Eutrophication (generic)	2.6570×10^{-5}	5.7735×10^{-5}	kg PO ₄ equivalent
Freshwater aquatic ecotoxicity	0.2872	0.2897	kg 1,4-dichlorobenzene equivalent
Human toxicity	3.6207	6.8614	kg 1,4 dichlorobenzene equivalent
Marine aquatic ecotoxicity	694	47	kg 1,4-dichlorobenzene equivalent
Ozone layer depletion (steady state)	0.8409×10^{-10}	1.8273×10^{-10}	kg cfc-11 equivalent
Photochemical oxidation (high oxides of nitrogen, NO _x)	1.6530×10^{-5}	3.5918×10^{-5}	kg ethylene equivalent
Terrestrial ecotoxicity	33	87	kg 1,4-dichlorobenzene equivalent

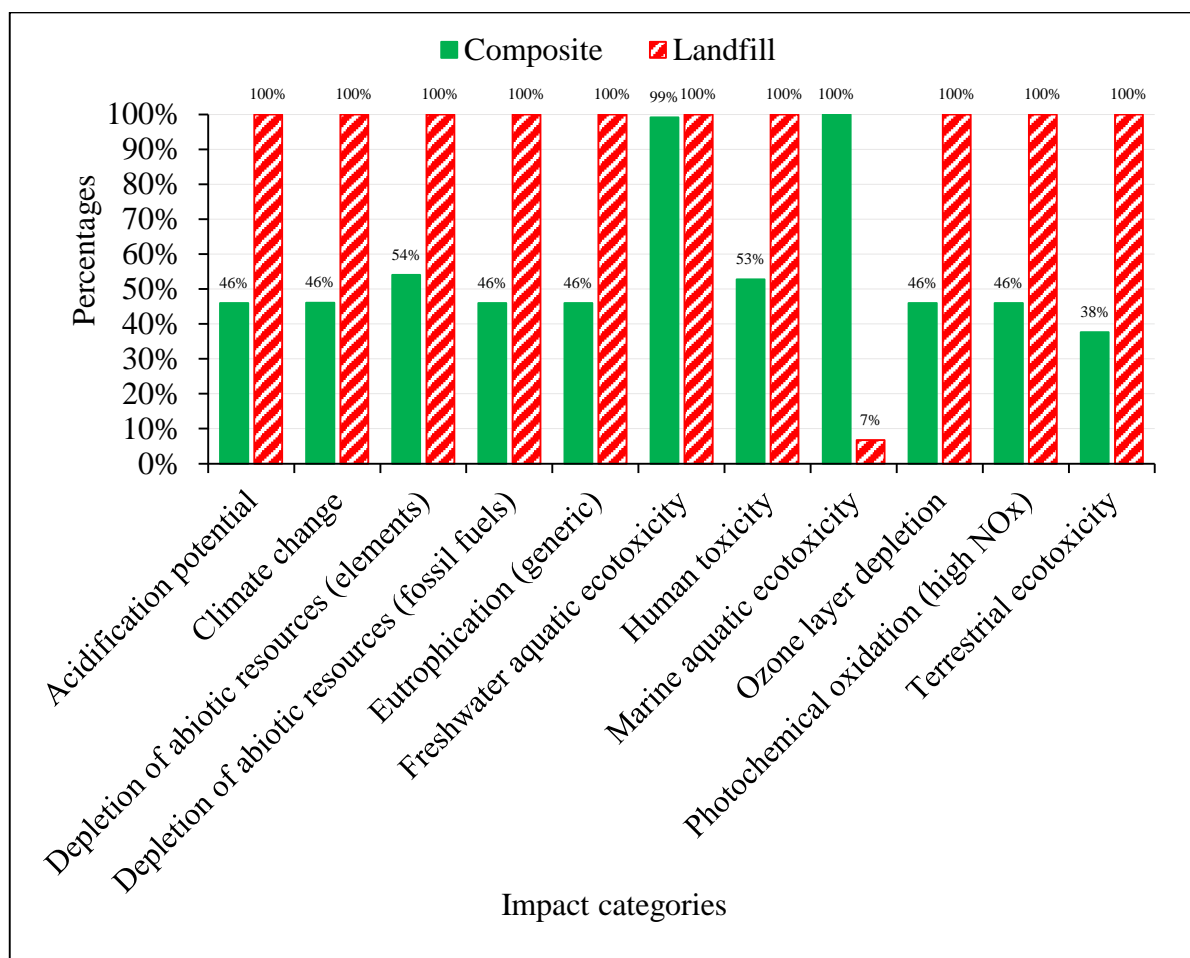
120

121 In figure 2 and table 3, composites and landfill routes were successfully analyzed by
 122 openLCA software using the CML-baseline method. The environmental impacts of composite
 123 and landfill are as follows: acidification potential 0.0002 and 0.0004 kg SO₂ eq., climate change
 124 0.1295 and 0.2808 kg CO₂ eq., depletion of abiotic resources (elements) 0.6511×10^{-5} and
 125 1.2054×10^{-5} kg antimony eq., depletion of abiotic resources (fossil fuels) 0.5454 and 1.1852
 126 mJ, eutrophication (generic) 2.6570×10^{-5} and 5.7735×10^{-5} kg PO₄-eq., freshwater aquatic
 127 ecotoxicity 0.2872 and 0.2897 kg 1,4-dichlorobenzene eq., human toxicity 3.6207 and 6.8614
 128 kg 1,4-dichlorobenzene eq., ozone layer depletion 0.8409×10^{-10} and 1.8273×10^{-10} kg cfc-11
 129 eq., photochemical oxidation (high NO_x) 1.6530×10^{-5} and 3.5918×10^{-5} kg ethylene eq.,
 130 terrestrial ecotoxicity 33 and 87 kg 1,4-dichlorobenzene eq., respectively. Except for impacts

131 on the marine aquatic ecosystem. The composite route had 694 kg 1,4-dichlorobenzene eq.,
 132 which was higher than the landfill route with 47 kg 1,4-dichlorobenzene eq.

133 3.2. Relative result

134 Relative result: This is found by dividing the amount of impact on each side of the two wet
 135 blue leather management routes by the maximum amount of that impact and multiplying by
 136 100 to get the relative result in percentage form, as shown in figure 3. The composite route
 137 has resulted in environmental impacts in acidification potential, climate change, depletion of
 138 abiotic resources (elements), depletion of abiotic resources (fossil fuels), eutrophication
 139 (generic), freshwater aquatic ecotoxicity, human toxicity, ozone layer depletion, photochemical
 140 oxidation (high NO_x), and terrestrial ecotoxicity. It has less impact than the landfill route. It is
 141 only in the impact on marine aquatic ecosystems that the composite route has a higher impact
 142 than landfills.



143

144 **Figure 3.** Relative result of life cycle assessment of composite based on ENR/wet blue leather.

145 **Conclusion**

146 The life cycle assessment of wet blue leather on the route between the landfill and
147 composites was successfully analyzed by openLCA software using the CML-baseline method.
148 The results concluded that the composite route from epoxidized natural rubber/wet blue leather
149 has a lower impact than the landfill route in almost every aspect except the marine aquatic
150 ecotoxicity. Therefore, the composite route should be a more suitable alternative to landfill.

151

152 **Worachai Techo:** Methodology, software, draft preparation, formal analysis, investigation,
153 visualization. **Laksamon Raksaksri:** Conceptualization, validation, writing—original, editing,
154 supervision, project administration. All authors have read and agreed to the published version
155 of the manuscript.

156

157 **Funding:** NRIIS number 179334 and grant no. FF7-710-64-36-24(F).

158

159 **Acknowledgments:** This work was supported by Suranaree University of Technology (grant
160 no. FF7-710-64-36-05(F), Thailand Science Research and Innovation (TSRI), and National
161 Science, Research, and Innovation Fund (NSRF) (NRIIS number 179334) (grant no. FF7-710-
162 64-36-24(F)).

163

164 **Conflicts of Interest:** “The authors declare no conflict of interest.”

165

166 **References**

- 167 1. Carbon figures show why hides must not go to waste. Available online: URL [https://vdl-](https://vdl-web.de/en/2021/02/03/carbon-figures-show-why-hides-must-not-go-to-waste-2/)
168 [web.de/en/2021/02/03/carbon-figures-show-why-hides-must-not-go-to-waste-2/](https://vdl-web.de/en/2021/02/03/carbon-figures-show-why-hides-must-not-go-to-waste-2/)
169 (accessed on 3 February 2024).
- 170 2. Ulya, M.; Arifuddin, A.L. and Hidayat, A.K. Life Cycle Assessment of Cow Tanned
171 Leather Products. In Proceedings of International Conference on Sustainable
172 Agriculture and Biosystem, West Sumatera, Indonesia, 25 November 2020.

- 173 3. Li, S. *et al.* Natural Rubber-Based Elastomer Reinforced by Chemically Modified
174 Multiscale Leather Collagen Fibers with Excellent Toughness. *ACS Sustainable Chem*
175 *Eng*, 2020, 8, 5091–5099.
- 176 4. Laurentia *et al.* Biodegradable Polymer Composite based on Recycled Polyurethane
177 and Finished Leather Waste. In *Proceedings of 2019 3rd International Conference on*
178 *Environmental Industrial and Energy Engineering*, Yinchuan, China, 19–21 September
179 2019.
- 180 5. Meyer *et al.* Comparison of the Technical Performance of Leather Artificial Leather
181 and Trendy Alternatives. *Coatings*, 2021, 11, 226.
- 182 6. Stefaniak, K.; Masek, A. and Jastrzebska, A. Biocomposites of Epoxidized Natural
183 Rubber Modified with Natural Substances. *Molecules*, 2022, 27, 7877.
- 184 7. Surana *et al.* Compression and fracture behavior of leather particulate reinforced
185 polymer composites. *Materials Research Express*, 2020, 7, 054006.
- 186 8. Meng, X. *et al.* Identification of the potential environmental loads of waste tire
187 treatment in China from the life cycle perspective. *Resources, Conservation &*
188 *Recycling*, 2023, 193, 106938.
- 189 9. Fela, K. *et al.* Present and prospective leather industry waste disposal. *A Polish Journal*
190 *of Chemical Technology*, 2011, 13&3, 53–55.
- 191 10. Wan, Y. *et al.* Informal landfill contributes to the pollution of microplastics in the
192 surrounding environment. *Environmental Pollution*, 2022, 293, 118586.

Proceedings

1 Effect of modified clay with zinc stearate on properties of natural rubber composites: 2 Cure characteristics, mechanical properties and Payne effect

3 Muna Muchcawech¹, Raymond Lee Nip², Yeampon Nakaramontri^{1*}

4 ¹Sustainable Polymer & Innovative Composites Material Research Group, Department of
5 Chemistry, Faculty of Science, King Mongkut's University of Technology Thonburi,
6 Bangkok, Thailand

7 ²Global Chemical Co., Ltd. Bangpoo Industrial Estate, Samutprakarn, Thailand

8 *Corresponding author: Yeampon Nakaramontri; E-mail: yeampon.nak@kmutt.ac.th

9 **Abstract:** Natural rubber (NR) composites filled with unmodified and modified clay with
10 chemical formation of zinc ions and stearic acid, namely zinc stearate, were prepared using an
11 internal mixer and a two-roll mill. The intrinsic properties of both clay types were
12 characterized through particle size analyzer and x-rays diffraction (XRD), while the cure
13 characteristics, mechanical properties and storage modulus following the Payne effect were
14 reported after the incorporation inside the NR matrix. It was found that the use of modified
15 clay showed the smaller particle size with exfoliation structure due to the increase band gap
16 among the clay layers. This causes well dispersion of modified clay within NR which further
17 induced chemical crosslinking reaction together with the comparable tensile properties and
18 Payne effect. This means the modification is successfully prepared and the improved
19 properties are established.

20 **Keywords:** Natural rubber; modified clay; Dispersion; Payne effect; Properties

21 1. Introduction

22 Nanomaterials in the rubber industry have attracted considerable attention as
23 reinforcing agents for elastomeric materials due to their outstanding improvements in various
24 properties compared to traditional composites. In addition to commonly used materials like
25 carbon black and silica, nanoclays are among the most widely utilized and extensively studied
26 fillers. Most commonly used nanoclays in polymers, such as montmorillonite, have a layered
27 structure, discovered by Dumour and Savetat [1]. Currently, it is popular to use nanoclays as
28 reinforcing agents in polymers due to their abundant natural availability and low cost. The
29 prominent feature is their platelet shape with a high aspect ratio and a nanosize thickness,
30 resulting in a high surface area. For this reason, polymers reinforced with nanoclays can
31 improve properties of mechanical, dynamic, adhesion, flame retardancy [2], gas permeability,
32 and thermal stability [3]. However, making a nanoclay composite without modification does
33 not significantly impact natural rubber (NR) because the surface of nanoclay tends to be
34 hydrophilic [4], whereas NR is a hydrophobic polymer. This mismatch may result in poor
35 dispersion and agglomeration within the rubber matrix.

36 Nevertheless, NR remains a highly appealing material due to its environmental
37 friendliness and outstanding performance characteristics, including resilience, elasticity,
38 abrasion resistance, efficient heat dispersion (minimizing heat build-up under friction), and
39 impact resistance [5]. To enhance dispersion in the rubber matrix, the most commonly used

40 technique is the cation exchange surface modification method. This process involves
41 exchanging ions between layers with organic cations, leading to the separation of clay
42 platelets, and allowing for easier intercalation and exfoliation. By exchanging of sodium
43 cations for organic cations (surfactants), the interlayer spacing expands [6], resulting in
44 improved dispersion, mechanical properties, and other characteristics. Sookyung *et al.*
45 prepared NR composites filled with octadecylamine-modified montmorillonite nanoclay
46 (OCMMT) using melt mixing processes. It was found that the modified clay improved
47 dispersion and distribution of clay inside NR matrix which further enhanced the degree of
48 rubber chains crosslinking and mechanical properties of the composites. Also, comparing the
49 NR/OCMMT nanocomposites with the unmodified clay, thermal stability and swellability
50 were significantly reduced due to good dispersion of silicate layer in rubber matrix [7]. In
51 addition, Hrachová *et al.* prepared NR nanocomposites filled with organoclay modified using
52 octadecyl trimethylammonium bromide (ODTMA) and the results showed improvement of
53 the mechanical properties in terms of tensile strength, elongation at break, tensile modulus,
54 and hardness. The dispersion of clay within the NR matrix indicated the intercalated and
55 exfoliated of an individual silicate layers [8]. Therefore, the use of modified clays has a
56 positive effect on the properties of rubber composites. The improved dispersion and
57 interaction of modified clays within the matrix enhanced mechanical properties, thermal
58 stability, and dynamic mechanical properties. These enhancements make the modified clay-
59 filled rubber composites suitable for a wide range of industrial applications.

60 The present research work is aimed to investigate the influence of unmodified clay and
61 modified clay with zinc stearate with natural rubber composites, on the properties of cure
62 characteristics, mechanical properties, and the Payne effect.

63 **2. Experimental**

64 **2.1 Materials**

65 Natural rubber (NR), grade STR5L (Standard Thai Rubber 5L), 1,2-Dihydro-2,2,4-
66 trimethylquinoline (TMQ) and N-Cyclohexylbenzothiazol-2-sulphenamide (CBS) were
67 purchased from Bossoftical Public Company Limited (Songkhla, Thailand). ULTRASIL
68 VN23 Silica and silane coupling agent TESPDP were obtained from Evonik Industries AG
69 (Wesseling, Germany). Modified clay is the modification of the bentonite clay with zinc
70 stearate using the technique of cation exchange involves replacing Na^+ ions in the clay with
71 Zn^{2+} ions from modifier. Zinc oxide (ZnO) and sulfur were provided by Global Chemical
72 Company Limited (Samut Prakan, Thailand). Stearic acid was purchased Imperial Chemical
73 Company Limited (Pathum Thani, Thailand). Diphenylguanidine (DPG) was purchased
74 Shenyang Sunnyjoint chemicals Company Limited (Liaoning, China).

75 **2.2 Preparation of the NR composites**

76 Preparation process of the NR composites filled with unmodified and modified clay
77 was initiated by the mastication of NR inside an internal mixer in order to reduce the viscosity
78 and surface tension of the NR matrix before adding other chemicals following the Table 1
79 following the published tire thread formulation. The total mixing operation was carried out
80 for approximately 12 min. The compounds were then passed on the two-roll mill for
81 improving the dispersion and distribution of the unmodified and modified clay throughout the

82 NR matrix. The NR composites were eventually pressed through the compression molding
83 following the rheometer testing.

84 **2.3 Particle size**

85 The particle size distribution (PSD) of the unmodified and modified clay powder was
86 determined by a Partica LA-960 (HORIBA Limited, Kyoto, Japan).

87 **2.4 X-ray diffraction**

88 X-ray diffraction (XRD) was performed on dried powder samples. The XRD patterns
89 were obtained using a Smart Lab SE (Rigaku Corporation, Tokyo, Japan) with Cu K α
90 radiation ($\lambda = 1.54 \text{ \AA}$). The samples were scanned at a rate of $0.05^\circ/\text{min}$ from 5° to 30° of 2θ .

91 **2.5 Cure characteristics**

92 Curing parameters, including scorch time (t_{s2}), optimum cure time (t_{90}), maximum and
93 minimum torque (M_H , M_L). The compounds were studied using the Rubber Process Analyzer
94 model RPA2000 (Alpha Technologies, Ohio, USA) at 150°C for 30 min.

95 **2.6 Tensile properties**

96 The tensile properties of NR composites filled with unmodified and modified clay
97 were determined using a universal testing machine (Zwick Z 1545, Zwick GmbH and Co.
98 KG, Ulm, Germany). Tests were carried out according to ISO 037 (Type 2), using a 500 N
99 load cell and 200 mm/min crosshead speed.

100 **2.7 Payne effect**

101 The Payne effects of NR composites filled with unmodified and modified clay were
102 evaluated using a RPA200 at a temperature of 100°C , frequency of 1 Hz and varying strains
103 in the range of 0.56– 100%.

104 **3. Results and discussion**

105 **3.1 Particles size and interaction among the clay layers**

106 Table 2 shows the average particles sizes of the unmodified and modified clay using
107 the chemical combination of the zinc ion (Zn^{2+}) and stearic acid. It is seen that the combination
108 of the bentonite clay with modifier represented the smaller of the particle size than the one
109 without modification for approximately 2 times. This can be referred to the increase of the
110 distance among the clay layer regarding the penetration of the Zn^{2+} -stearic acid linkages. This
111 clarifies through the demonstration of the XRD results seen in Figure 1. Considering of the
112 appearance peaks among 2θ of $20\text{-}30^\circ$ which assign to the reflection of the X-rays radiation
113 through the clay layer, it is seen that the modified clay exhibited smaller of each peak than the
114 unmodified which disappeared at the 2θ of $20\text{-}25^\circ$. This means that the clay layer had distance
115 in a proper position which X-ray diffraction cannot be detected. In addition, the XRD pattern
116 of unmodified clay shows a highest peak at a 2θ angle of 7° , corresponding to an interlayer
117 spacing of 1.26 nm. In contrast, the modified clay shows a highest peak at a 2θ angle of 6° ,
118 corresponding to an interlayer spacing of 1.48 nm. This indicates that the interlayer spacing

119 of the modified clay is greater than that of the unmodified clay, confirming the intercalation
120 of zinc stearate into the clay layers.

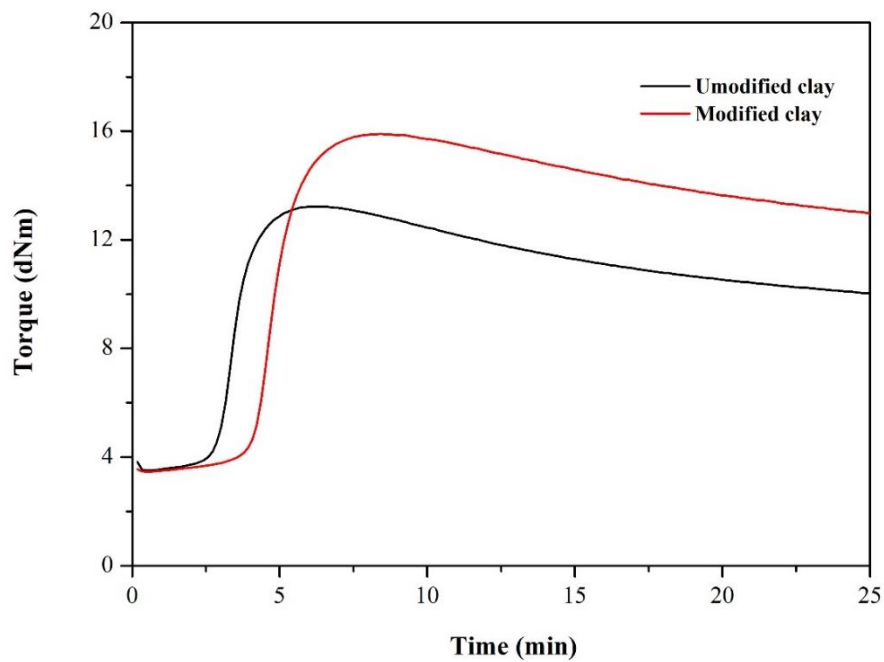
121 **3.2 Cure characteristics**

122 Figure 2 presents the cure curves of the NR composites filled with unmodified and
123 modified clay. It is clearly seen that both curves show the reversion behavior due to the poor
124 thermal stability of the NR regarding thermos-oxidative degradation. However, the addition
125 of the modified clay slightly retarded the reversion due to the dispersion and distribution of
126 clay within the NR matrix. In addition, Table 3 summarizes the cure properties of both
127 composites, and it was found that the composites showed increase of the scorch time (T_{s2}) and
128 cure time (T_{90}) after using the modified clay. This was explained by the thermal insulation of
129 the clay layers which prevent thermal expansion inside the NR matrix and therefore the
130 vulcanization propagation was slower since the modified clay had better dispersion degrees.
131 Additionally, the higher M_H-M_L , which is assigned to the estimated crosslink density inside
132 the bulk NR composites, is due to the zinc ions released from zinc stearate. These ions
133 facilitate the crosslinking reaction by coordinating with sulfur atoms, thereby promoting their
134 interaction with the rubber chains. This coordination allows for more efficient bonding
135 between adjacent rubber molecules regarding the roles of zinc stearate which can act as the
136 plasticizer for clay dispersion and also activator for increasing crosslink density.

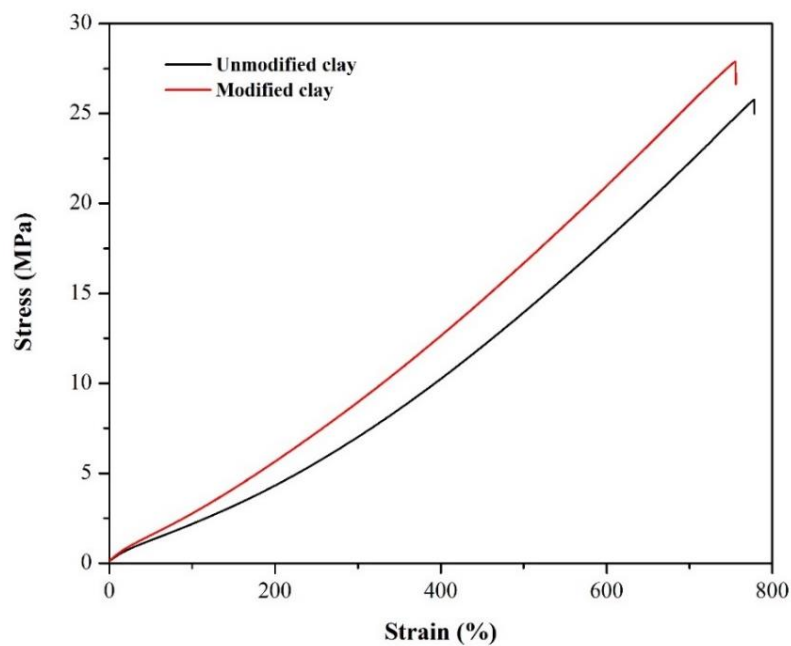
137 **3.3 Mechanical properties and Payne effect**

138 The mechanical properties, including tensile strength, 100% and 300% moduli, and
139 elongation at break of the NR composites filled with different types of clays, are demonstrated
140 in Figure 3, Figure 4 shows the Payne effect and summarizes the data in Table 4. It is seen in
141 Figure 3 that the well dispersion and distribution of the modified clay relative the unmodified
142 clay caused improved significantly the improved 100 and 300% moduli. This means that the
143 composites had high potential to retard the stress applying deformation due to superior
144 reinforcement efficiency. Also, considering the tensile strength (T.S.) and elongation at break
145 (E.B.) of the NR composites, it was observed that the uses of the modified clay provide
146 increase of the T.S. with lower E.B. This correlates to the explanation that the incased tensile
147 strength and stiffness can lower than elasticity of the NR matrix and therefore the E.B. had
148 decreased. Also, it is seen that the NR composites with modified clay showed lower of the
149 Payne effect which mainly referred to the smaller of the clay agglomeration inside the NR
150 composites. Zinc stearate, acting as a clay modifier, reduces friction between the rubber
151 matrix and filler materials, such as clay particles. This friction reduction facilitates better clay
152 dispersion and distribution within the rubber matrix, thereby enhancing mechanical properties.

153 **3.4. Figures and Tables**



154 **Figure 1** The X-ray diffraction (XRD) patterns of unmodified and modified clay to clarify the
 155 distribution of clay particles.



156 **Figure 2** Cure curves of the NR composites filled with unmodified and modified clay.

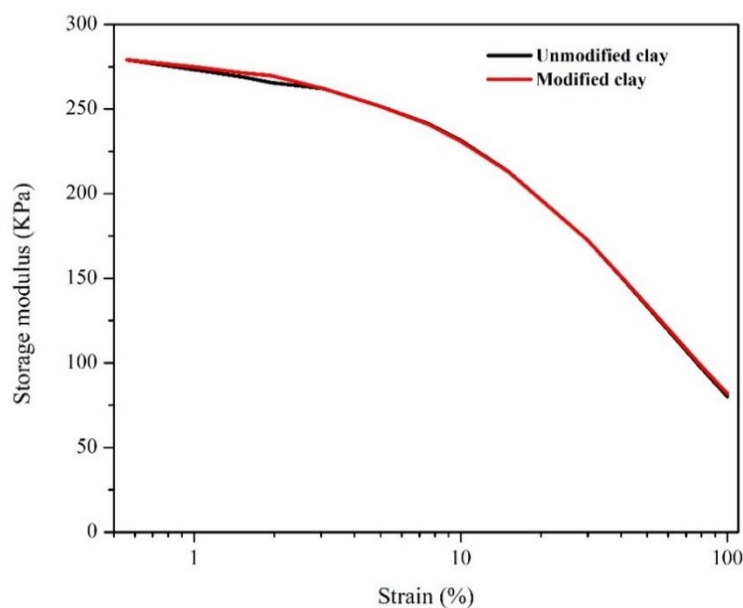
157 **Figure 3** Stress-strain curves of the NR composites filled with unmodified and modified clay.

158 **Figure 4** Payne effect of the NR composites filled with unmodified and modified clay.

159 **Table 1** Formulation of the NR composites filled with unmodified and modified clay.

Ingredients	Content (phr)
Natural rubber	100
Silica+TESPT	60
Clay/Modified clay	10
ZnO	3
Stearic acid	1
Antidegradant	1
Accelerator	2.6
Sulfur	1.5

160 **Table 2** Particle size of the unmodified and modified clay.



Name	Particle size (μm)
Unmodified clay	8.65
Modified clay	4.01

161 **Table 3** Cure characteristics of the NR composites filled with unmodified and modified clay.

Cure characteristics	NR composites filled with unmodified and modified clay	
	Unmodified clay	Modified clay
T_{s2} (min)	3.10	4.43
T_{90} (min)	4.44	6.21
M_H (dNm)	13.23	15.90
M_L (dNm)	3.50	3.46
M_H-M_L (dNm)	9.73	12.44

163 **Table 4** Tensile properties with the indication of the Payne effect of the NR composites filled
 164 with unmodified and modified clay.

Mechanical properties	NR composites filled with unmodified and modified clay	
	Unmodified clay	Modified clay
Tensile strength (MPa)	25.78 ± 0.54	27.89 ± 0.12
Elongation at break (%)	778.25 ± 9.72	755.53 ± 10.26
100 % Modulus (MPa)	2.19 ± 0.03	2.77 ± 0.03
300 % Modulus (MPa)	7.02 ± 0.08	8.96 ± 0.07
Payne effect (KPa)	199.27	197.34

165 **4. Conclusion**

166 The NR composites filled with unmodified and modified clay were carried out by
 167 focusing on the improved properties of the NR composites regarding the cure characteristic,
 168 mechanical properties, and Payne effect for examining the dispersion and distribution of the
 169 clay inside the NR matrix. It was found that the modification of the clay layer with the
 170 chemical coupling among Zn²⁺ and stearic acid had smaller of the particle sizes and higher
 171 distance among the clay layers. This achievement causes the higher of the crosslinking density
 172 for the covalent bonding among the NR molecules and also the modulus and tensile strength
 173 of the NR composites relative to the one with unmodified clay. Although the elongation at
 174 break was slight lower, the Payne effect showed that improved dispersion of the clay can be
 175 gained after the modification process. Therefore, the present work can further apply for the
 176 rubber manufacturing which would use the clay as the secondary filler in order to improve the
 177 properties of the composites.

178 **Author Contributions:** M.M.: Conception and Design, Methodology, Validation, Data
 179 Analysis, Writing—original draft preparation, R.M.N.: Conceptualization, Methodology,
 180 Validation, Formal analysis, Y.N.: Visualization, Supervision, Formal analysis, Writing—
 181 review and editing, Funding acquisition. All authors have read and agreed to the published
 182 version of the manuscript.

183 **Funding:** This research project is supported by King Mongkut's University of Technology
 184 Thonburi (KMUTT), Thailand Science Research Innovation (TSRI) and National Science,
 185 Research and Innovation Fund (NSRF) Fiscal year (2024).

186 **Acknowledgments:** The authors gratefully acknowledge the financial support from the King
 187 Mongkut's University of Technology Thonburi (KMUTT), Bangkok, in the form of KMUTT
 188 Research Fund for the financial support and equipment. Also, Thailand Science Research and
 189 Innovation (TSRI) and National Science, Research and Innovation Fund (NSRF) Fiscal year
 190 2024 was acknowledged.

191 **Conflicts of Interest:** "The authors declare no conflict of interest."

192 **References**

- 193 1. Gao, F. (2004). Clay/polymer composites: the story. *Materials today*, 7(11), 50-55.
- 194 2. Kotal, M., & Bhowmick, A. K. (2015). Polymer nanocomposites from modified clays:
195 Recent advances and challenges. *Progress in Polymer Science*, 51, 127-187.
- 196 3. Sookyung, U., Nakason, C., Thaijaroen, W., & Vennemann, N. (2014). Influence of
197 modifying agents of organoclay on properties of nanocomposites based on natural
198 rubber. *Polymer testing*, 33, 48-56.
- 199 4. Kumari, N., & Mohan, C. (2021). Basics of clay minerals and their characteristic
200 properties. *Clay Clay Miner*, 24, 1-29.
- 201 5. Mooibroek, H., & Cornish, K. (2000). Alternative sources of natural rubber. *Applied*
202 *microbiology and biotechnology*, 53, 355-365.
- 203 6. Maiti, P., Yamada, K., Okamoto, M., Ueda, K., & Okamoto, K. (2002). New
204 polylactide/layered silicate nanocomposites: role of organoclays. *Chemistry of*
205 *materials*, 14(11), 4654-4661.
- 206 7. Sookyung, U., Thaijaroen, W., & Nakason, C. (2014). Influence of modifying
207 organoclay on the properties of natural rubber/organoclay nanocomposites. *Journal of*
208 *Composite Materials*, 48(16), 1959-1970.
- 209 8. Hrachová, J., Komadel, P., & Chodák, I. (2008). Effect of montmorillonite
210 modification on mechanical properties of vulcanized natural rubber composites.
211 *Journal of Materials Science*, 43, 2012-2017.

Proceedings

1 **Food-contact potential of polylactic acid/natural rubber (PLA/NR)** 2 **packaging films**

3 **Nuengruthai Chuayrueng, Cattaleeya Pattamaprom***

4 Department of Chemical Engineering, Faculty of Engineering, Thammasat School of Engineering, Thammasat University,
5 Pathum Thani 12120, Thailand
6 email: cattalee@engr.tu.ac.th

7 **Abstract:**

8 This research investigated the food-contact potential of polylactic acid/natural rubber (PLA/NR)
9 packaging films at NR contents ranging from 0-25 wt% in terms of chemical migration from the
10 films. The overall migration test was studied by immersing samples in four different food simulants –
11 ethanol 10% (v/v), acetic acid 3% (w/v), ethanol 95% (v/v), and vegetable oil – under both short-term
12 and long-term food contact conditions (OM0 and OM2). The specific migration test was studied using
13 an ED-XRF technique to identify a specific migrant in ethanol 95% (v/v). VOCs that migrated from
14 the films were identified using HS/GC-MS. The result indicated that the PLA/NR films at all NR
15 contents had overall migration amounts well below the EU-regulated standard migration in all food
16 simulants. Chemical analysis revealed the presence of CaCO₃ (used as a nonstick agent for NR).
17 According to the VOCs test, No VOCs were released when the PLA/NR films were incubated at 40
18 °C. This result suggested that PLA/NR films at NR contents up to 25%wt could be used for food
19 packaging applications for all types of food at short and long storage times at cold and ambient
20 temperatures.

21 **Keywords:** PLA/NR film; Food contact; Migration test; Overall migration; Specific migration

22 **1. Introduction**

23 Plastic production has grown faster than any other material since 1970s. If the current
24 trend continues, primary plastic production could reach 1,100 million tonnes by 2050. About
25 36% of those are used for packaging, which includes single-use plastics for food and beverage
26 containers. Almost 98% of these single-use plastics are made from fossil fuels. After being
27 disposed of, around 85% of this plastic ends up in landfills or as unregulated waste^[1]. Although
28 many countries promote the use of bio-based plastics as a replacement for petroleum-based
29 plastics, the high production costs remain a challenge. According to 2021 statistics,
30 biodegradable plastics comprised only 1.5% of the world's plastic production and 2.3% of
31 Europe's plastic production^[2]. Polylactic acid (PLA) is the cheapest bio-based plastic that has
32 been approved for food packaging^{[3], [4]}. However, it has limitations in terms of its toughness,
33 brittleness, and thermal stability^[5]. To enhance its toughness, PLA has been blended with bio-
34 or petroleum-based plastics^[6]. Our research group extensively investigated on the blends of
35 PLA and natural rubber (NR) for packaging applications because NR is a fully biopolymer with
36 outstanding elasticity, tensile strength, and toughness. Even though NR is cheaper than PLA,
37 packaging films made from PLA/NR still have a higher cost than petroleum-based plastics.
38 Therefore, it is of interest to expand the application ranges of PLA/NR to food-contact
39 applications. So far, there is a lack of studies investigating the food contact potential of
40 PLA/NR films in terms of consumer safety. Therefore, the food-contact potential of PLA/NR
41 blends could be a challenge and is worth investigation.

42 2. Experimental

43 Materials

44 PLA Pellets 4043D was purchased from Nature Works Co. Ltd., USA. Natural Rubber (STR
45 grade 5L) was purchased from Innovation Group (Thailand) Ltd. Ethanol (95%) (a food
46 simulant) and CaCO₃ were purchased from Chemipan Corporation Co., Ltd. Acetic acid (≥
47 99.7%) (a food simulant) was purchased from J.T. Baker (USA). Helium (99.999%) was used
48 as the carrier gas for GC-MS.

49 Migration test

50 This research aimed to study the overall and specific migrations from the PLA/NR films at NR
51 contents ranging from 0 – 25 wt%. The migration test was carried out according to regulation
52 (EU) No 10/2011 on plastic materials and articles intended to come into contact with food, EN
53 1186-2:2022 on test methods used for overall migration in vegetable oils, and EN 1186-3:2022
54 on test methods for overall migration in evaporable simulants.

55 Overall migration test

56 The PLA/NR films were cut and immersed in food simulants using a film to food simulant ratio
57 of 6 dm²/kg at cold or ambient temperatures for short (OM0) and long (OM2) durations, where
58 the contact conditions for OM0 and OM2 are 30 mins and 10 days, respectively, at 40 °C. The
59 food simulants for aqueous and acidic foods are 10% ethanol and 3% acetic acid, respectively.
60 The primary food simulant for oily food which contains free fats at the surface is vegetable oil,
61 and 95% ethanol could also be used as a vegetable oil substitute^[7]. The overall migration
62 amount was calculated by Eq. (1) and the test was conducted twice to ensure accuracy.

$$63 \quad \text{Overall migration} \left(\frac{mg}{dm^2} \right) = \frac{m_s - m_b}{\text{film surface area}} \quad (1)$$

64 where m_s and m_b represent the dried weight of remaining residue in the food simulant and in
65 the blank, respectively. For the high-boiling point food simulant (olive oil), the films were sent
66 out to a testing service company due to the unavailability of testing equipment.

67 Specific migration test

68 Specific migration from PLA/NR films was evaluated by ED-XRF technique. The migrant
69 solutions from ethanol 95% food simulant were chosen for this test because of their highest
70 OM values. A Shimadzu Energy-Dispersive X-ray Fluorescence (EDX-7000) was used to
71 analyze for inorganic components. The specific migration was conducted twice to ensure
72 accuracy.

73 Surface morphology test

74 This test aimed to observe the changes in surface morphology of PLA/NR films before and
75 after being exposed to food simulants at 40 °C for 10 days (OM2). The macroscopic surfaces
76 were observed by using a digital camera, while the microscopic images were obtained by a
77 Field Emission Scanning Electron Microscope (FE-SEM). Before the SEM observation, the
78 specimens were sputtered with gold under vacuum.

Proceedings

79 Analysis of volatile organic compounds (VOCs)

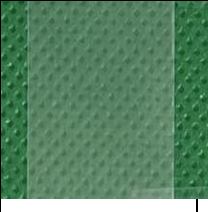
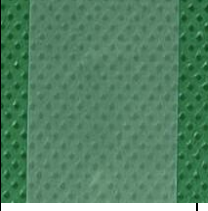
80 To identify the VOCs emitted from the PLA/NR films, the films were weighed and packed in
 81 a headspace vial of a GC-MS. The vial was then incubated with a headspace autosampler at the
 82 incubation temperatures (40 °C) for 15 minutes. The VOCs test was conducted twice to ensure
 83 accuracy.

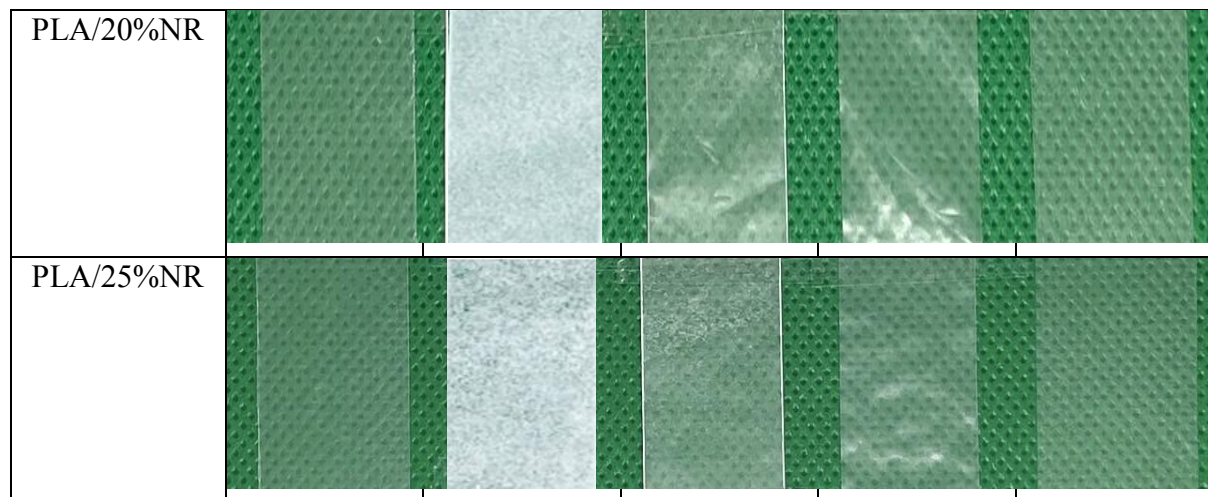
84 3. Results and Discussion

85 The changes in surface morphology of PLA/NR films after exposure to food simulants

86 For a short-term exposure (OM0), all films remained visually unchanged, except for slight
 87 wrinkles found in the case of films in 95% ethanol. For the longer exposure time of 10 days
 88 (OM2), the visual appearance of the film surfaces is shown in Table 1. As can be seen, the
 89 surface of PLA film remained smooth when exposed to all food simulants; however, it turned
 90 slightly opaque due to some degree of water and ethanol adsorption. On the other hand, the
 91 PLA/NR films turned white in 3% acetic acid solution (Table 1) with a significant change in
 92 surface roughness, especially at higher NR contents. In 95% ethanol, the macroscopic view of
 93 all films (Table 1) reveals some wrinkles and slight increase in surface roughness without
 94 significant rubber agglomeration.

95 Table 1. The visual appearance of films after exposure to food simulants at OM2 condition

Film samples	Food simulants at OM2 condition				
	Before Test	Acetic Acid 3%	Ethanol 10%	Ethanol 95%	Vegetable oil
Neat PLA					
PLA/10%NR					
PLA/15%NR					



96 **Overall migration result**

97 The overall migration from PLA/NR films at NR contents ranging from 0 – 25 wt% was
 98 evaluated in four different food simulants: 10% ethanol (v/v), 3% acetic acid (w/v), 95%
 99 ethanol (v/v), vegetable oil – under both short-term (OM0) and long-term (OM2) food contact
 100 conditions. The overall migration results are shown in Table 2. As can be seen, the overall
 101 migrations of films in all types of food simulants at both OM0 and OM2 are in the range of 0
 102 – 4.7 mg/dm² (Table 2), which are well below the overall migration limit (OML = 10 mg/dm²)
 103 required by the Regulation (EU) No 10/2011.

104 Table 2. The overall migration levels of PLA and PLA/NR films under OM2 condition.

Film samples	Overall migration levels (mg/dm ²)			
	3% Acetic acid	10% ethanol	95% ethanol	Vegetable Oil
Neat PLA	0	0.1	1.6	0
PLA/10%NR	0	0.1	2.2	0
PLA/15%NR	0	0.5	3.0	4.7
PLA/20%NR	0	0.6	3.3	0
PLA/25%NR	0	0.9	3.9	0

105 **Specific migration results**

106 The substances that migrated from PLA/NR films at OM2 were identified using XRF and
 107 SEM-EDX for inorganic migrants. The XRF results indicated that the migrants from the films
 108 with higher NR contents contained higher amounts of Ca element. The source of Ca element
 109 was expectedly from CaCO₃ used as a non-stick agent for NR. This could be a result of better
 110 PLA chain mobility in ethanol (higher swelling) than in water. The higher Ca content detected
 111 at higher %NR reveals that the migrants came partly from the migration of CaCO₃ from the
 112 films.

113 **Analysis of volatile organic compounds (VOCs)**

114 The non-polar VOCs were analyzed by a headspace GC-MS at the incubation temperatures of
 115 40 °C. It was found that no non-polar VOCs were detected from any films incubated at 40 °C.

116 Conclusion

117 The investigation into chemical migration from PLA/NR packaging films, with NR contents
118 ranging from 0 to 25 wt%, aimed to assess their suitability for food contact and offer insights
119 for product enhancement. The analysis included overall migration (OM), specific migration
120 (SM), and volatile organic compounds (VOCs) emitted from the films. Overall, the OM and
121 SM levels of all PLA/NR films remained well below the maximum limit specified by the EU-
122 regulated standard across all food simulants under both OM0 and OM2. Regardless of low
123 migration levels, the PLA/NR films turned white in aqueous solutions (3% acetic acid and 10%
124 ethanol) potentially posing a perception issue and restricting their application range. Chemical
125 analysis revealed the presence of CaCO₃ (used as a nonstick agent for NR). Notably, no VOCs
126 were released from all PLA/NR films at room temperature up to 40 °C. These findings
127 suggested that all PLA/NR films, with NR contents up to 25 wt% exhibit very low overall
128 migration without any toxic substances, thus making them suitable for food packaging across
129 various food types and storage durations at both cold and ambient temperatures.

130 Authors' contributions

131 1. N. Chuayrueng: experimental planning and methodology, data analysis, original draft
132 preparation and revision

133 2. C. Pattamaprom: conceptualization, data analysis, manuscript writing, editing and proof-
134 reading, funding acquisition

135 All authors have read and agreed to the published version of the manuscript.

136 Data availability

137 Supplementary Data are available in supplementary materials.

138 Funding

139 This research was funded by Thammasat School of Engineering (TSE), Thammasat University,
140 2024. In addition, this research was partially supported by Fundamental Fund (FF2567),
141 Thailand Science Research and Innovation (TSRI), Thailand, 2024, and the research unit in
142 polymer rheology and processing, Thammasat University.

143 Conflicts of Interest

144 The authors declare no conflict of interest.

Proceedings

145 References

- 146 1. UNEP. Our planet is choking on plastic. 2023 [cited 2023; Available from:
147 <https://www.unep.org/interactives/beat-plastic-pollution/>.
- 148 2. Europe, P. Plastics – the Facts 2022 An Analysis of European Plastics Production,
149 Demand and Waste Data. 2022; Available from: [https://plasticseurope.org/knowledge-](https://plasticseurope.org/knowledge-hub/plastics-the-facts-2022/)
150 [hub/plastics-the-facts-2022/](https://plasticseurope.org/knowledge-hub/plastics-the-facts-2022/).
- 151 3. Chen, W.-Y., T. Suzuki, and M. Lackner, Handbook of climate change mitigation and
152 adaptation. 2017: Springer International Publishing Cham, Switzerland.
- 153 4. Van den Oever, M., et al., Bio-based and biodegradable plastics: facts and figures: focus
154 on food packaging in the Netherlands. 2017: Wageningen Food & Biobased Research.
- 155 5. Chanthot, P., N. Kerddonfag, and C. Pattamaprom, The effect of peroxide on the film
156 blowing stability and rheological properties of polylactic acid blown films. Journal of
157 Hunan University Natural Sciences, 2021. 48(8).
- 158 6. Nofar, M., et al., Poly (lactic acid) blends: Processing, properties and applications.
159 International journal of biological macromolecules, 2019. 125: p. 307-360.
- 160 7. EU, COMMISSION REGULATION (EU) No 10/2011 of 14 January 2011 on plastic
161 materials and articles intended to come into contact with food, EU, Editor. 2011. p. 1-
162 89.